

SURFACE WAVES IN RANDOMLY PERTURBED DISCRETE MODELS*

JOSSELIN GARNIER[†] AND BASANT LAL SHARMA[‡]

Abstract. We study the propagation of surface waves across structured surfaces with random, localized inhomogeneities. A discrete analogue of the Gurtin–Murdoch model is employed, and surface elasticity, in contrast to bulk elasticity, is captured by distinct point masses and elastic constants for nearest-neighbor interactions parallel to the surface. Expressions for the surface wave reflectance and transmittance, as well as the radiative loss, are provided for every localized patch of point mass perturbation on the surface. As the main result in the article, we provide the statistics of surface wave reflectance and transmittance and the radiative loss for an ensemble of random mass perturbations, independent and identically distributed with mean zero, on the surface. In the weakly scattering regime, the mean radiative loss is found to be proportional to the size of the perturbed patch, to the variance of the mass perturbations, and to an effective parameter that depends on the continuous spectrum of the unperturbed system. In the strongly scattering regime, the mean radiative loss is found to depend on another effective parameter that depends on the continuous spectrum, but not on the variance of the mass perturbations. Numerical simulations are found in quantitative agreement with the theoretical predictions for several illustrative values of the surface structure parameters.

Key words. random perturbations, lattice dynamics, discrete Laplacian, Gurtin–Murdoch, multiscale analysis

MSC codes. 34F05, 60H10, 34C15, 37K60

DOI. 10.1137/24M165510X

1. Introduction. Surface waves play an important role at small length scales in physical structures, in addition to their role in traditional engineering systems [42, 23, 9, 2, 12]. However, surfaces and coatings are not perfect [26, 45], and this leads to several challenges along with their diverse applications at nano-scale, though sometimes defects are intentionally crafted for desired signal transmission. The high frequency wave scattering, due to steps and serrations on crystal [22, 31], involves the discreteness of structure, and the perturbations influence the dynamical and wave phenomena [17, 11, 50]. Indeed, the physical understanding of surfaces and interfaces has evolved over several decades [48, 29, 44, 47]. The nano-scale effects are becoming increasingly relevant in current science such as the case of functional nanomaterials and miniaturized structures [30, 28, 20] for their elastic, electronic, and thermal properties. On the other hand, the presence of randomness at small scales has led to an impact on the fundamental physical principles [1, 8].

Restricting to the classical theories, within the continuum models of surface elasticity, [18, 19] proposed an independent set of constitutive relations on the surface in addition to the ones defined in the bulk; this modeling can be interpreted as an elastic

*Received by the editors April 17, 2024; accepted for publication (in revised form) September 25, 2024; published electronically January 9, 2025.

<https://doi.org/10.1137/24M165510X>

Funding: This work was supported by Engineering and Physical Sciences Research Council grant EP/R014604/1. Part of the work of the second author was partially supported by a Simons Foundation grant.

[†]Centre de Mathématiques Appliquées, Ecole Polytechnique, Institut Polytechnique de Paris, Palaiseau, 91120, France (josselin.garnier@polytechnique.edu).

[‡]Department of Mechanical Engineering, Indian Institute of Technology Kanpur, Kanpur, 208016, UP, India (bls@iitk.ac.in).

membrane glued on the material surface and is referred as the Gurtin–Murdoch model. Recently, a discrete Gurtin–Murdoch model was introduced by [13], wherein a comparison of the surface waves between the continuous Gurtin–Murdoch model and the discrete framework of lattice dynamics is also provided within the kinematic assumption of antiplane shear deformation (out-of-plane motion). The problem of scattering of such surface waves, due to specific surface inhomogeneities, has been tackled in [41, 39, 40], where it is found that the energy flux of surface waves is “leaked” at the defects in the form of bulk waves. In more general situations and complicated lattices, indeed, it is quite common to find surface (phonon) bands in the crystal models [7, 21, 48], though the calculations along the lines of [39, 40] are less convenient.

Specifically, in this article, a prototype of surface wave propagation in a semi-infinite square lattice half plane representing the surface of a crystalline structure is analyzed in the presence of random perturbations of the masses at the boundary. The specific lattice model adopted, based on that introduced in [13], is shown schematically in Figure 1. The techniques developed in the general problem of discrete scattering on uniform square lattices [33, 34, 35, 24], without additional surface structure, do assist in carrying forward the analysis to such structured half planes, while our recent work on the one dimensional lattice model [16] paved way for the choice of the simplest form of the half plane model. As a preliminary result, the exact solution of the problem of scattering of surface waves due to a patch of size L of perturbed masses is provided using the lattice Green’s function for the assumed structure; the latter corresponds to the solution of the discrete Helmholtz equation in the semi-infinite lattice with a point source at the surface [40]. The reflection and transmission coefficients for surface wave propagation, from one side of the patch to another, can then be obtained via the inversion of an $L \times L$ matrix. Together with a conservation of energy relation, the expressions of the reflection and transmission coefficients give in turn a formula for the radiative loss, namely the fraction of incident energy flux that is “leaked” at the interface in the form of bulk waves. The main result concerns the question about the dependence of the physically important effects of randomness in the surface ma-

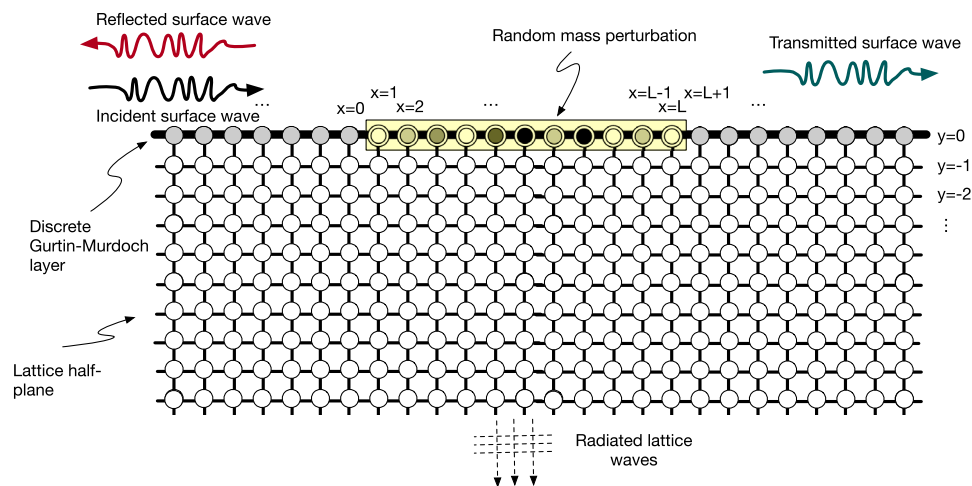


FIG. 1. Schematic of surface wave transmission in a randomly perturbed Gurtin–Murdoch lattice model: A square lattice half plane endowed with a boundary with structure containing certain random mass defects in a finite region of size L sites.

terial parameters. This is answered for the surface wave transmission problem by an application of stochastic and multiscale analysis [14]. Such an approach has already been successfully applied to wave propagation in randomly perturbed systems such as acoustic, elastic, or electromagnetic waves, including wave propagation in randomly perturbed waveguides [15, 4, 5] and surface wave propagation in a randomly perturbed continuous half-space [10, 6]. In the case of the randomly perturbed discrete Gurtin–Murdoch model addressed in this paper, it is possible to study the regime where the relative standard deviation of the mass perturbations is small and the size L of the perturbed patch is large so that the cumulative effects of the mass perturbations onto the propagation of an incident surface wave are of order one. A system of stochastic differential equations for the reflection and transmission coefficients as functions of the size of the perturbed patch can be obtained, which takes into account all relevant phenomena, including the coupling with radiative and evanescent modes. This system gives in turn the expressions of the moments of the reflection and transmission coefficients and the radiative loss. An inspection of these expressions reveals that, in the weakly scattering regime, the mean radiative loss is proportional to the size of the randomly perturbed patch, to the variance of the mass perturbations, and to an effective parameter that depends on the continuous spectrum of the unperturbed system. In the strongly scattering regime, the mean radiative loss depends on another effective parameter, but not on the variance of the mass perturbations. The numerical calculations suggest that the dependence of transmittance and radiative loss on the incident wave frequency is nonmonotone in surface wave band for each instance of perturbation, while the mean values are monotone mostly. In general, the results on transmittance and radiative loss are highly susceptible to the choice of values of physical parameters associated with the unperturbed surface structure.

The present article is organized as follows. The discrete Gurtin–Murdoch lattice model incorporating the surface structure is formulated in section 2 along with a short description of the associated surface waves. Section 2 provides the complete eigenbasis for the difference operator characterizing the unperturbed one dimensional semi-infinite lattice model closely related to the lattice half plane. Section 2 also contains details on the modal expansion of the solution of the unperturbed equation of motion of the lattice half plane with surface structure. The exact solution of the scattering problem of surface waves, due to a finite size of the patch, of possibly large, mass perturbation on the boundary, appears in section 3 after solving the discrete Lippmann–Schwinger equation. The expressions of reflection and transmission coefficients are provided in section 3 using the Green’s function for point source on the boundary of the half plane. Section 3 also contains the energy conservation theorem, which provides the statement of distribution of the energy flux of the incident surface wave into reflected and transmitted surface waves apart from the waves radiated into the half plane. The main result of this article appears in section 4 concerning the effects on scattering of surface waves due to randomness in small mass perturbation on a finite sized patch on the boundary. Proof of the main result is provided in section 5 using a multiscale analysis of the the modal expansion of the solution of the perturbed equation of motion, dealing with the role of the evanescent and radiative modes. After concluding remarks, a list of references and two appendices complete the article.

Mathematical preliminaries. Let \mathbb{Z} denote the set of integers, let \mathbb{Z}^2 denote $\mathbb{Z} \times \mathbb{Z}$, and let \mathbb{Z}^- denote the set of negative integers. The definitions

$$(1.1a) \quad \mathbb{H} := \{(\mathbf{x}, \mathbf{y}) \in \mathbb{Z}^2 : \mathbf{y} \leq 0\},$$

$$(1.1b) \quad \mathring{\mathbb{H}} := \{(\mathbf{x}, \mathbf{y}) \in \mathbb{Z}^2 : \mathbf{y} \in \mathbb{Z}^-\}, \quad \partial\mathbb{H} := \{(\mathbf{x}, \mathbf{y}) \in \mathbb{Z}^2 : \mathbf{y} = 0\}$$

represent the square lattice half plane with boundary, without boundary, and the boundary itself, respectively. Let \mathbb{R} denote the set of real numbers, and let \mathbb{C} denote the set of complex numbers. For $z \in \mathbb{C}$, $\operatorname{Re} z \in \mathbb{R}$ denotes the real part, $\operatorname{Im} z \in \mathbb{R}$ denotes the imaginary part, \bar{z} denotes the complex conjugate $\operatorname{Re} z - i \operatorname{Im} z$ of z , $|z|$ denotes the modulus, and $\arg z$ denotes the principal argument. The square root function has the usual branch cut in the complex plane running from $-\infty$ to 0. The symbol \mathbb{T} denotes the unit circle (as a counterclockwise contour) in the complex plane. If f is a differentiable, real- or complex-valued, function, then f' denotes the derivative of f . The decoration $\check{}$ is used to represent the modal amplitudes in contrast to $\hat{}$, $\hat{}$ for the incident wave. The subscript 0 typically accompanies entities related to the surface wave, while the subscript s appears with surface structure parameters. The usage of \mathbf{x}, \mathbf{y} is restricted to emphasize the lattice coordinates; in particular, $\mathbf{x}, \mathbf{y} \in \mathbb{Z}$. The symbol \mathfrak{z} is reserved for a complex variable.

2. Lattice model and completeness of eigenfunctions.

2.1. Discrete Gurtin–Murdoch lattice model. Consider the unperturbed lattice model, ignoring the yellow patch in Figure 1, which provides a schematic representation of the lattice model with surface structure and point mass perturbation. Within the paradigm of the out-of-plane displacement field of a lattice structure, the equation of motion on $\mathring{\mathbb{H}}$, the portion of lattice half plane away from its boundary, is

$$(2.1a) \quad \Delta \mathbf{u}_{\mathbf{x}, \mathbf{y}} = \ddot{\mathbf{u}}_{\mathbf{x}, \mathbf{y}}, \quad (\mathbf{x}, \mathbf{y}) \in \mathring{\mathbb{H}},$$

where $\Delta \mathbf{u}_{\mathbf{x}, \mathbf{y}} \equiv \mathbf{u}_{\mathbf{x}+1, \mathbf{y}} + \mathbf{u}_{\mathbf{x}-1, \mathbf{y}} + \mathbf{u}_{\mathbf{x}, \mathbf{y}+1} + \mathbf{u}_{\mathbf{x}, \mathbf{y}-1} - 4\mathbf{u}_{\mathbf{x}, \mathbf{y}}$,

while the equation of motion of the particles on the lattice half plane boundary $\partial\mathbb{H}$, as the counterpart of (2.1a), is

$$(2.1b) \quad \alpha_s(\mathbf{u}_{\mathbf{x}+1, \mathbf{y}} + \mathbf{u}_{\mathbf{x}-1, \mathbf{y}} - 2\mathbf{u}_{\mathbf{x}, \mathbf{y}}) + \mathbf{u}_{\mathbf{x}, \mathbf{y}-1} - \mathbf{u}_{\mathbf{x}, \mathbf{y}} = m_s \ddot{\mathbf{u}}_{\mathbf{x}, \mathbf{y}}, \quad \mathbf{x} \in \mathbb{Z}, \mathbf{y} = 0,$$

where $m_s > 0$ represents the possibly distinct mass of particles at $\partial\mathbb{H}$ and $\alpha_s > 0$ denotes the elastic constants for nearest-neighbor interactions parallel to the surface. Equations (2.1a), (2.1b) are postulated as the discrete Gurtin–Murdoch lattice model, following the naming convention used in [13, 40], analogous to the continuous model [18], and the physical scaling described in section 3 of [13]. Note that [18] provided the boundary conditions for the continuum model in case of statics, while their linearized version for the scalar case of antiplane motion appears as equation (2) in [13].

We consider the time-harmonic problem, with $\omega > 0$ as the frequency of excitation of the wave field as shown schematically in Figure 1, so that

$$(2.2a) \quad \Delta \mathbf{u}_{\mathbf{x}, \mathbf{y}} + \omega^2 \mathbf{u}_{\mathbf{x}, \mathbf{y}} = 0, \quad (\mathbf{x}, \mathbf{y}) \in \mathring{\mathbb{H}},$$

and

$$(2.2b) \quad \alpha_s(\mathbf{u}_{\mathbf{x}+1, \mathbf{y}} + \mathbf{u}_{\mathbf{x}-1, \mathbf{y}} - 2\mathbf{u}_{\mathbf{x}, \mathbf{y}}) + \mathbf{u}_{\mathbf{x}, \mathbf{y}-1} - \mathbf{u}_{\mathbf{x}, \mathbf{y}} + m_s \omega^2 \mathbf{u}_{\mathbf{x}, \mathbf{y}} = 0, \quad \mathbf{x} \in \mathbb{Z}, \mathbf{y} = 0,$$

corresponding to (2.1a) and (2.1b), respectively.

The above equations, (2.2a) in $\mathring{\mathbb{H}}$ and (2.2b) in $\partial\mathbb{H}$, allow a surface wave band for the values of α_s and m_s such that $\alpha_s < m_s$ [13]; see [40] for an elementary justification

of this condition, and, in particular, note that the case $m_s = \alpha_s = 1$ does not permit such a surface wave band. Indeed, it is easy to see, after the substitution of

$$(2.3) \quad \mathbf{u}_{\mathbf{x},\mathbf{y}} = e^{ik_0\mathbf{x} + \eta(k_0)\mathbf{y}}, \quad k_0 \in (-\pi, \pi) \setminus \{0\},$$

in (2.2a), (2.2b), that the common description of surface waves is satisfied, provided $\omega \equiv \omega(k_0)$ and $\eta \equiv \eta(k_0) > 0$ are implicitly obtained from the two coupled equations

$$(2.4) \quad \omega^2 = 4\sin^2(k_0/2) + 2 - 2\cosh \eta, \quad m_s\omega^2 = 4\alpha_s\sin^2(k_0/2) + 1 - e^{-\eta}.$$

Thus, \mathbf{u} in (2.3) represents a *surface wave mode* of dimensionless wavenumber $k_0 \in (-\pi, \pi) \setminus \{0\}$ that decays exponentially into \mathbb{H} with an attenuation coefficient $\eta(k_0)$. Note that

$$(2.5) \quad \omega(k_0) \in (0, \omega_{\max}) =: \mathcal{P}_s, \quad k_0 \in (-\pi, \pi) \setminus \{0\},$$

where ω_{\max} is given by

$$(2.6) \quad \omega_{\max} = \sqrt{(-b_s + \sqrt{b_s^2 - 4a_s c_s}) / (2a_s)},$$

with $a_s = m_s(m_s - 1)$, $b_s = -8\alpha_s m_s + 4\alpha_s + 4m_s + 1$,
 $c_s = 16\alpha_s^2 - 16\alpha_s - 4$.

Note that $\omega_{\max} < 2$ according to the conditions (2.4) whenever the surface wave band exists. For each given $\omega \in \mathcal{P}_s$, there exist two surface wave modes of the form (2.3), which can be classified as a left-going and a right-going wave based on the sign of the propagation of energy flux. The group velocity of the surface wave (2.3) with wave number $k_0 \in (-\pi, \pi) \setminus \{0\}$ is [7]

$$(2.7) \quad v_s(k_0) := \frac{d}{d\xi} \omega(\xi)|_{\xi=k_0} = \frac{\sin k_0}{\omega(k_0)} \frac{\alpha_s + (e^{2\eta(k_0)} - 1)^{-1}}{m_s + (e^{2\eta(k_0)} - 1)^{-1}}.$$

The surface wave (2.3) carries energy flux towards $\mathbf{x} \rightarrow +\infty$ (resp., $-\infty$) when $k_0 \in (0, \pi)$ (resp., $-k_0 \in (0, \pi)$) as $v_s(k_0) > 0$ (resp., $v_s(k_0) < 0$).

Before proceeding to the main results, for the randomly perturbed discrete Gurtin–Murdoch model with localized mass perturbations on sites in $\partial\mathbb{H}$, certain results regarding the spectral properties of the difference operator involved in (2.2a), (2.2b) on \mathbb{H} are needed. In retrospect, it is convenient to study a reduced one dimensional lattice model on $\mathbb{Z}^- \cup \{0\}$ at first.

2.2. Completeness of eigenfunctions for a (reduced) one dimensional semi-infinite lattice model. Suppose that ω belongs to the regime when a surface wave mode (2.3) exists on \mathbb{H} and (2.2a), (2.2b) are satisfied, i.e., $\omega \in (0, \omega_{\max}) \subset (0, 2)$, where ω_{\max} is given by (2.6). Following Appendix A of [10], the objective is to show that the solution of the unperturbed system can be expanded on a complete system of eigenfunctions, which represent both the propagative modes, that is, surface mode and the radiative modes, and the evanescent modes.

We first introduce the unnormalized functions ψ_γ which appear in the expressions of the eigenfunctions.

2.2.1. Unnormalized functions. For any $\gamma \in \mathbb{R}$, we denote by $\psi_\gamma : \mathbb{Z}^- \cup \{0\} \rightarrow \mathbb{C}$ the unique solution of the second-order difference equation

$$(2.8a) \quad (\Delta_1 + \omega^2)\psi_\gamma(\mathbf{y}) = \gamma\psi_\gamma(\mathbf{y}), \quad \mathbf{y} \in \mathbb{Z}^-,$$

$$(2.8b) \quad \psi_\gamma(\mathbf{y} - 1) - \psi_\gamma(\mathbf{y}) + m_s \omega^2 \psi_\gamma(\mathbf{y}) = \alpha_s \gamma \psi_\gamma(\mathbf{y}), \quad \mathbf{y} = 0,$$

$$(2.8c) \quad \psi_\gamma(\mathbf{y}) = 1, \quad \mathbf{y} = 0,$$

where Δ_1 is the one dimensional discrete Laplacian

$$(2.8d) \quad \Delta_1 \psi(\mathbf{y}) \equiv \psi(\mathbf{y} + 1) + \psi(\mathbf{y} - 1) - 2\psi(\mathbf{y}), \quad \mathbf{y} \in \mathbb{Z}, \psi : \mathbb{Z} \rightarrow \mathbb{C}.$$

The function ψ_γ has the following form.

If $\gamma \neq \omega^2$, then there exists a unique $\beta \neq 0$ such that $\text{Re } \beta \geq 0, \text{ Im } \beta \geq 0$, and $e^\beta + e^{-\beta} - 2 + \omega^2 = \gamma$. Then $\psi_\gamma = A_\gamma e^{\beta \mathbf{y}} + (1 - A_\gamma) e^{-\beta \mathbf{y}}$, where $A_\gamma = (-\alpha_s \gamma - 1 + m_s \omega^2 + e^\beta) / (e^\beta - e^{-\beta})$ (so that the two boundary conditions (2.8b), (2.8c) hold).

If $\gamma = \omega^2$, then $\psi_\gamma = 1 + A_\gamma \mathbf{y}$, where $A_\gamma = (m_s - \alpha_s) \omega^2$ (so that (2.8b), (2.8c) hold).

- (i) If $\gamma \in (\omega^2 - 4, \omega^2)$, we have $\beta = \pm i\zeta, \zeta \in (-\pi/2, \pi/2)$ with $2 \cos \zeta - 2 + \omega^2 = \gamma$. For $\mathbf{y} \leq 0$, $\psi_\gamma = A_\gamma e^{i\zeta \mathbf{y}} + \overline{A_\gamma} e^{-i\zeta \mathbf{y}}$, with $A_\gamma = \frac{1}{2} + \frac{i}{2 \sin \zeta} (-\cos \zeta + \alpha_s \gamma + 1 - m_s \omega^2)$, which yields

$$(2.9) \quad \psi_\gamma(\mathbf{y}) = \frac{1}{\sin \zeta} ((m_s \omega^2 - \alpha_s \gamma - 1) \sin \zeta \mathbf{y} + \sin \zeta (\mathbf{y} + 1)).$$

Thus, ψ_γ is bounded on \mathbb{Z}^- .

- (ii) If $\gamma < \omega^2 - 4$ or $\gamma > \omega^2$, then ψ_γ is exponentially growing on \mathbb{Z}^- as $\mathbf{y} \rightarrow -\infty$ because $A_\gamma \neq 1$ except for one value $\gamma_0 > \omega^2$ (assuming $\alpha_s < m_s$) which is such that $A_{\gamma_0} = 1$. This value γ_0 yields an eigenfunction $\psi_{\gamma_0}(\mathbf{y}) = e^{\beta_0 \mathbf{y}}$ where $\beta_0 > 0$ is such that

$$(2.10) \quad \omega^2 = 2 + \gamma_0 - 2 \cosh \beta_0, \quad m_s \omega^2 = \alpha_s \gamma_0 + 1 - e^{-\beta_0}.$$

Thus, ψ_{γ_0} is square summable on \mathbb{Z}^- .

2.2.2. Orthonormal eigenfunctions. We consider the weighted l^2 space of typical $u : \mathbb{Z}^- \cup \{0\} \rightarrow \mathbb{C}$ with the norm defined by

$$(2.11) \quad \|u\|_2^2 := \alpha_s |u_0|^2 + \sum_{\mathbf{y} \in \mathbb{Z}^-} |u_{\mathbf{y}}|^2,$$

and the associated inner product defined by

$$(2.12) \quad \langle u, v \rangle := \alpha_s u_0 \overline{v_0} + \sum_{\mathbf{y} \in \mathbb{Z}^-} u_{\mathbf{y}} \overline{v_{\mathbf{y}}}.$$

In this context, recall that $\alpha_s > 0$ so that the above definitions are nondegenerate. Inspired by the equations (2.8a), (2.8b), (2.8c), consider the definition

$$(2.13) \quad (\mathcal{L}u)_{\mathbf{y}} := \begin{cases} \Delta_1 u_{\mathbf{y}} + \omega^2 u_{\mathbf{y}} & \text{if } \mathbf{y} \in \mathbb{Z}^-, \\ \frac{1}{\alpha_s} (u_{-1} - u_0 + m_s \omega^2 u_0) & \text{if } \mathbf{y} = 0. \end{cases}$$

By a direct calculation, it is found that the operator \mathcal{L} defined by (2.13) is self-adjoint in l^2 , i.e.,

$$\langle u, \mathcal{L}v \rangle = \langle \mathcal{L}u, v \rangle$$

for all $u, v \in l^2$ with weighted inner product defined by (2.12).

A sketch of the (standard) proof of spectral properties of \mathcal{L} is as follows. Let us fix some positive integer D . If one considers the domain $[-D, 0] \cap \mathbb{Z}$ with Dirichlet boundary condition at $y = -D$ instead of $(-\infty, 0] \cap \mathbb{Z}$, then the operator \mathcal{L} is self-adjoint and compact (equivalent to a $D \times D$ matrix in this case). By the spectral theorem for $D \times D$ symmetric matrices there exists an orthonormal basis consisting of eigenfunctions of \mathcal{L} . The eigenvalues are simple $\gamma_{j,D}$ and the eigenfunctions $\phi_{\gamma_{j,D}}$ (proportional to $\psi_{\gamma_{j,D}}$) are orthogonal (the eigenvalues are simple because, for any γ , the solution of $\mathcal{L}\psi = \gamma\psi$ with $\psi(0) = 1$ is unique). One can then proceed as in [10, Appendix A]. By taking the limit $D \rightarrow +\infty$ one gets that the operator \mathcal{L} on l^2 has a discrete spectrum made of one isolated eigenvalue γ_0 and a continuous spectrum on $(\omega^2 - 4, \omega^2)$.

PROPOSITION 2.1. *Any function $u \in l^2$ (with weighted inner product (2.12)) can be expanded as*

$$(2.14) \quad u_{\mathbf{y}} = \check{u}_{\gamma_0} \phi_{\gamma_0}(\mathbf{y}) + \int_{\omega^2-4}^{\omega^2} \check{u}_{\gamma} \phi_{\gamma}(\mathbf{y}) d\gamma,$$

with the modal amplitudes given by

$$(2.15a) \quad \check{u}_{\gamma_0} = \langle u, \phi_{\gamma_0} \rangle,$$

$$(2.15b) \quad \check{u}_{\gamma} = \langle u, \phi_{\gamma} \rangle, \quad \gamma \in (\omega^2 - 4, \omega^2),$$

and eigenmodes given by

$$(2.15c) \quad \phi_{\gamma_0}(\mathbf{y}) = \sqrt{\rho(\gamma_0)} \psi_{\gamma_0}(\mathbf{y}),$$

$$(2.15d) \quad \phi_{\gamma}(\mathbf{y}) = \sqrt{\rho(\gamma)} \psi_{\gamma}(\mathbf{y}), \quad \gamma \in (\omega^2 - 4, \omega^2),$$

where

$$(2.15e) \quad \rho(\gamma_0) = \frac{1}{\alpha_s + (e^{2\beta_0} - 1)^{-1}},$$

$$(2.15f) \quad \rho(\gamma) = \frac{2 \sqrt{(\omega^2 - \gamma)(\gamma - \omega^2 + 4)}^{-1}}{\pi \left(1 + \frac{(\gamma(2\alpha_s - 1) + \omega^2(1 - 2m_s))^2}{(\omega^2 - \gamma)(\gamma - \omega^2 + 4)} \right)}, \quad \gamma \in (\omega^2 - 4, \omega^2).$$

We also have the Parseval relation

$$(2.16) \quad \|u\|_2^2 = |\check{u}_{\gamma_0}|^2 + \int_{\omega^2-4}^{\omega^2} |\check{u}_{\gamma}|^2 d\gamma$$

for all $u \in l^2$.

Proposition 2.1 shows that, after suitable normalization of ψ_{γ} obtained in section 2.2.1, a function in l^2 can be expanded on the complete set of eigenfunctions ψ_{γ} , $\gamma \in (\omega^2 - 4, \omega^2) \cup \{\gamma_0\}$. An alternative way to arrive at the normalization of ψ_{γ} is provided in Appendix A.

2.3. Modal expansion of the solution of the unperturbed equation of motion. In view of Proposition 2.1, the solution $\mathbf{u} : \mathbb{H} \rightarrow \mathbb{C}$, which satisfies the equation of motion (2.2a) with the surface condition (2.2b) on $\partial\mathbb{H}$ for all $\mathbf{x} \in \mathbb{Z}$, can be expanded as the superposition of orthonormal modes obtained in section 2.2.2:

$$(2.17) \quad \mathbf{u}_{\mathbf{x},\mathbf{y}} = \check{\mathbf{u}}_{\gamma_0}(\mathbf{x})\phi_{\gamma_0}(\mathbf{y}) + \int_{\omega^2-4}^{\omega^2} \check{\mathbf{u}}_{\gamma}(\mathbf{x})\phi_{\gamma}(\mathbf{y})d\gamma, \quad (\mathbf{x}, \mathbf{y}) \in \mathbb{H},$$

$$(2.18) \quad \text{with } \check{\mathbf{u}}_{\gamma_0}(\mathbf{x}) = \langle \mathbf{u}_{\mathbf{x},\cdot}, \phi_{\gamma_0} \rangle,$$

$$(2.19) \quad \check{\mathbf{u}}_{\gamma}(\mathbf{x}) = \langle \mathbf{u}_{\mathbf{x},\cdot}, \phi_{\gamma} \rangle, \quad \gamma \in (\omega^2 - 4, \omega^2),$$

using the weighted inner product defined by (2.12). Note that $\{\mathbf{u}_{\mathbf{x},\mathbf{y}}\}_{\mathbf{y} \in \mathbb{Z}^-}$ belongs to l^2 for each $\mathbf{x} \in \mathbb{Z}$ and, as mentioned before, we assume that $\omega \in \mathcal{P}_s = (0, \omega_{\max})$ (2.5).

The modal amplitudes in (2.17) satisfy the uncoupled difference equations

$$(2.20) \quad \check{\mathbf{u}}_{\gamma}(\mathbf{x} + 1) + \check{\mathbf{u}}_{\gamma}(\mathbf{x} - 1) + (\gamma - 2)\check{\mathbf{u}}_{\gamma}(\mathbf{x}) = 0, \quad \mathbf{x} \in \mathbb{Z}.$$

(i) If $\gamma \in (0, 4)$ then $\check{\mathbf{u}}_{\gamma}(\mathbf{x})$ has the form

$$\check{\mathbf{u}}_{\gamma}(\mathbf{x}) = ae^{ik(\gamma)\mathbf{x}} + be^{-ik(\gamma)\mathbf{x}}, \quad \mathbf{x} \in \mathbb{Z},$$

with

$$(2.21) \quad k(\gamma) = \arccos\left(1 - \frac{\gamma}{2}\right) \in (0, \pi), \quad \gamma \in (0, 4),$$

which shows that it is a propagative mode (the mode e^{ikx} is right-going on $\partial\mathbb{H}$, and e^{-ikx} is left-going on $\partial\mathbb{H}$).

(ii) If $\gamma < 0$ then $\check{\mathbf{u}}_{\gamma}(\mathbf{x})$ has the form

$$\check{\mathbf{u}}_{\gamma}(\mathbf{x}) = ae^{k(\gamma)\mathbf{x}} + be^{-k(\gamma)\mathbf{x}}, \quad \mathbf{x} \in \mathbb{Z},$$

with

$$(2.22) \quad k(\gamma) = \operatorname{arcosh}\left(1 - \frac{\gamma}{2}\right) = \ln\left(1 - \frac{\gamma}{2} + \frac{1}{2}\sqrt{\gamma(\gamma - 4)}\right) > 0, \quad \gamma < 0,$$

which shows that it is an evanescent mode.

To summarize, the discrete eigenvalue $\gamma_0 > \omega^2$ corresponds to a propagative mode, addressed as a surface wave mode (2.3) in section 2; the continuous spectrum has a propagative (radiative) part for $\gamma \in (0, \omega^2)$ and an evanescent part for $\gamma \in (\omega^2 - 4, 0)$.

Remark 2.2. For the discrete eigenvalue γ_0 , the attenuation coefficient β_0 in (2.10) corresponds to $\eta(k_0)$, and the wave number $k(\gamma_0)$ in (2.21) corresponds to k_0 in the surface wave mode (2.3). For the continuous spectrum with a propagative (radiative) part $\gamma \in (0, \omega^2)$, the wave numbers $\zeta \equiv \zeta(\gamma)$ in (2.9) and $k \equiv k(\gamma)$ in (2.21) correspond to the wave vectors $(k, \zeta) \in \mathbb{R}^2$ of bulk lattice waves, which have the form $e^{ikx+i\zeta y}$ [7, 33, 40] and satisfy the bulk dispersion relation $\omega^2 = 4 \sin^2 \frac{1}{2}k + 4 \sin^2 \frac{1}{2}\zeta$.

3. Exact solution on \mathbb{H} for arbitrary localized mass perturbation on $\partial\mathbb{H}$.

Suppose L is a given positive integer representing the size of patch on $\partial\mathbb{H}$ containing the mass defect. Let $\mu_{\mathbf{x}}$ describe the relative perturbation in mass at the lattice site $(\mathbf{x}, 0) \in \partial\mathbb{H}$. For $\mathbf{x} \in \{1, 2, \dots, L-1, L\}$ as there is a mass defect $\mu_{\mathbf{x}}m_s$, the mass of particle is $m_s(1 + \mu_{\mathbf{x}})$ in place of m_s in (2.2b). Note that the case of arbitrarily large perturbation in point masses associated with surface structure is permitted as long as the mass of individual particles remains positive.

We use $u_{\mathbf{x},\mathbf{y}}$ to represent the scattered field in response to an incident surface wave mode $\hat{\mathbf{u}}_{\mathbf{x},\mathbf{y}}$ for all $(\mathbf{x}, \mathbf{y}) \in \mathbb{H}$; naturally, the total field on \mathbb{H} is given by $\mathbf{u}_{\mathbf{x},\mathbf{y}} = u_{\mathbf{x},\mathbf{y}} + \hat{\mathbf{u}}_{\mathbf{x},\mathbf{y}}$. We assume that $\omega \in \mathcal{P}_s = (0, \omega_{\max})$ (2.5), that is, ω belongs to the regime when a surface wave mode (2.3) can exist in the unperturbed lattice model, where ω_{\max} is given by (2.6).

We consider a propagative (surface) wave mode incident from the left side of the surface patch on $\partial\mathbb{H}$ between $x = 1$ and $x = L$ (see yellow patch and wave schematic in Figure 1):

$$(3.1) \quad \widehat{u}_{x,y} = \hat{a} e^{ik_0x + \eta(k_0)y}, \quad k_0 \in (0, \pi),$$

where $\hat{a} \in \mathbb{C}$ is the amplitude; we assume that $\hat{a} \neq 0$.

We consider the equation of motion (2.2a) with the surface condition (2.2b) on $\partial\mathbb{H}$ satisfied by the total field $u_{x,y} + \widehat{u}_{x,y}$ for all $x \leq 0$ and $x \geq L+1$ and the surface condition with perturbed masses, i.e., $\alpha_s(u_{x+1,y} + u_{x-1,y} - 2u_{x,y}) + u_{x,y-1} - u_{x,y} + m_s(1 + \mu_x)\omega^2 u_{x,y} + \alpha_s(\widehat{u}_{x+1,y} + \widehat{u}_{x-1,y} - 2\widehat{u}_{x,y}) + \widehat{u}_{x,y-1} - \widehat{u}_{x,y} + m_s(1 + \mu_x)\omega^2 \widehat{u}_{x,y} = 0$ is satisfied for $x \in [1, L] \cap \mathbb{Z}$ and $y = 0$. As the equation of motion (2.2a) on \mathbb{H} with the surface condition (2.2b) on $\partial\mathbb{H}$ is satisfied by the incident wave \widehat{u} , therefore we find that the scattered wave field $u_{x,y}$ needs to satisfy (2.2a) on \mathbb{H} and at $y = 0$,

$$(3.2) \quad \alpha_s(u_{x+1,y} + u_{x-1,y} - 2u_{x,y}) + u_{x,y-1} - u_{x,y} + m_s\omega^2 u_{x,y} = \sum_{j=1}^L \delta_{x,j} f_j \quad \forall x \in \mathbb{Z},$$

where

$$(3.3) \quad f_j := -m_s\omega^2 \mu_j (u_{j,0} + \widehat{u}_{j,0}), \quad j = 1, \dots, L.$$

By inspection of (2.2a) and (3.2), it is clear that the solution can be expressed in terms of a Green's function. In particular, we consider the Green's function $\mathcal{G}_{x,y}$ for all $(x, y) \in \mathbb{H}$ that satisfies (2.2a), (2.2b) with a point source $\delta_{x,0}\delta_{y,0}$. The Kronecker delta is defined by

$$(3.4) \quad \delta_{x,n} := 0, \text{ if } x \neq n, \quad \text{and} \quad \delta_{x,n} := 1, \text{ if } x = n, \quad x, n \in \mathbb{Z}.$$

The Green's function \mathcal{G} satisfies the following equations:

$$(3.5a) \quad (\mathcal{G}_{x+1,y} + \mathcal{G}_{x-1,y}) + \mathcal{G}_{x,y+1} + \mathcal{G}_{x,y-1} - 4\mathcal{G}_{x,y} + \omega^2 \mathcal{G}_{x,y} = 0, \quad (x, y) \in \mathring{\mathbb{H}},$$

$$(3.5b) \quad \alpha_s(\mathcal{G}_{x+1,0} + \mathcal{G}_{x-1,0} - 2\mathcal{G}_{x,0}) + \mathcal{G}_{x,-1} - \mathcal{G}_{x,0} + \omega^2 m_s \mathcal{G}_{x,0} = \delta_{x,0}, \quad (x, 0) \in \partial\mathbb{H}.$$

The solution of the above system of equations (3.5) can be found in terms of a contour integral as the function $\mathcal{G}: \mathbb{H} \rightarrow \mathbb{C}$ given by

$$(3.6) \quad \mathcal{G}_{x,y} = \frac{1}{2\pi i} \int_{\mathbb{T}} \frac{\lambda^{-y}(\mathfrak{z}) \mathfrak{z}^{|x|-1}}{\mathfrak{R}_s(\mathfrak{z})} d\mathfrak{z}, \quad (x, y) \in \mathbb{H},$$

where \mathbb{T} denotes the counterclockwise unit circle contour in the complex plane, and

$$(3.7) \quad \begin{aligned} \mathfrak{R}_s(\mathfrak{z}) &= \lambda(\mathfrak{z}) + \mathfrak{F}_s(\mathfrak{z}), \quad \lambda(\mathfrak{z}) = \frac{\mathfrak{r}(\mathfrak{z}) - \mathfrak{h}(\mathfrak{z})}{\mathfrak{r}(\mathfrak{z}) + \mathfrak{h}(\mathfrak{z})}, \\ \mathfrak{h}(\mathfrak{z}) &= \sqrt{\mathfrak{Q}(\mathfrak{z}) - 2}, \quad \mathfrak{r}(\mathfrak{z}) = \sqrt{\mathfrak{Q}(\mathfrak{z}) + 2}, \quad \mathfrak{Q}(\mathfrak{z}) = 4 - \mathfrak{z} - \mathfrak{z}^{-1} - (\omega + i\varepsilon)^2, \\ \text{and } \mathfrak{F}_s(\mathfrak{z}) &= m_s\omega^2 - 1 + \alpha_s(\mathfrak{z} + \mathfrak{z}^{-1} - 2), \end{aligned}$$

with $\varepsilon > 0$ representing a vanishingly small absorption [33]. To obtain (3.6) from (3.5), we first replace ω by $\omega + i\varepsilon$ in (3.5) and seek the solution $\mathcal{G} \equiv \mathcal{G}(\varepsilon)$ that exponentially decays at infinity. The application of transform $\mathcal{G}_y^F(\mathfrak{z}) = \sum_{x \in \mathbb{Z}} \mathcal{G}_{x,y} \mathfrak{z}^{-x}$ facilitates finding that (1) $\mathcal{G}_y^F, y \in \mathbb{Z}^- \cup \{0\}$, is analytic in an annulus \mathcal{A} such as the one shown schematically in Figure 2 containing the unit circle \mathbb{T} , (2) by (3.5a), $\mathcal{G}_y^F = \mathcal{G}_0^F \lambda^{-y}$,

where λ (3.7) is analytic and nonvanishing in the same annulus \mathcal{A} , (3) by (3.5b), \mathcal{G}_0^F satisfies $\mathfrak{K}_s \mathcal{G}_0^F = 1$, where \mathfrak{K}_s (3.7) also does not vanish in \mathcal{A} , in particular on \mathbb{T} . The formula (3.6) follows using the analyticity of $\lambda^{-y}/\mathfrak{K}_s$ in the integrand of the contour integral on \mathbb{T} and Cauchy’s residue theorem. See section 8(a) in [40] for few more details regarding the Green’s function; see also section 5(c) in [40] and section 2.2 in [33] regarding the definitions that appear in (3.7).

Remark 3.1. Note that $\mathcal{G}_{x,y}$ (3.6) decays exponentially as $|\mathbf{x}|, |\mathbf{y}| \rightarrow \infty$ on \mathbb{H} under the assumption $\varepsilon > 0$. As $\varepsilon \rightarrow 0+$, the scattering solution, which satisfies radiation conditions [32] in the present two dimensional case, is recovered; see also [27], where the choice of sign in the imaginary part of the spectral parameter in the resolvent of the discrete Laplacian operator is clarified.

Let

$$(3.8) \quad \mathfrak{z}_0 := e^{ik_0},$$

where k_0 is the incident surface wave number in (3.1). Due to the presence of absorption $\varepsilon > 0$, \mathfrak{z}_0 lies inside the unit disk in complex plane \mathbb{C} , i.e., $|\mathfrak{z}_0| < 1$. Moreover, according to the definition in (3.7), $\lambda(\mathfrak{z}_0) = \lambda(\mathfrak{z}_0^{-1}) = e^{-\eta(k_0)}$.

Remark 3.2. Note that $\mathfrak{F}_s(\mathfrak{z}) = \mathfrak{F}_s(\mathfrak{z}^{-1})$ and $\lambda(\mathfrak{z}) = \lambda(\mathfrak{z}^{-1})$ so that $\mathfrak{K}_s(\mathfrak{z}) = \mathfrak{K}_s(\mathfrak{z}^{-1})$. Also note that $\mathfrak{K}_s(\mathfrak{z}_0) = 0$ and $\widehat{\mathbf{u}}_{x,0} = \widehat{\mathfrak{z}}_0^x$ according to (3.1), (3.8), and, in general, $\widehat{\mathbf{u}}_{x,y} = \widehat{\mathfrak{z}}_0^x \lambda^{-y}(\mathfrak{z}_0)$ using the definition in (3.7).

Remark 3.3. In connection with the eigenfunctions stated earlier, especially (2.15e), (2.15f), note that

$$(3.9) \quad \rho(\gamma_0) = \frac{(\mathfrak{z}_0 - \mathfrak{z}_0^{-1})}{\mathfrak{z}_0 \mathfrak{K}'_s(\mathfrak{z}_0)}, \quad \rho(\gamma) = \frac{1}{\pi} \frac{\text{Im } \lambda_\gamma}{|\mathfrak{K}_s(\mathfrak{z}_\gamma)|^2},$$

where $\lambda_\gamma \equiv \lambda(\mathfrak{z}_\gamma)$ using the following mappings:

$$(3.10) \quad \gamma \equiv \gamma(\mathfrak{z}) = 2 - \mathfrak{z} - \mathfrak{z}^{-1} \text{ and } \mathfrak{z}_\gamma \equiv \mathfrak{z}(\gamma) \text{ such that } |\mathfrak{z}_\gamma| < 1.$$

In addition to Remark 2.2, note that $\mathfrak{z}_{\gamma_0} = \mathfrak{z}_0$ defined in (3.8) while $\gamma(\mathfrak{z}_0) = \gamma_0$. In this context, see Appendix A as well.

Using the formula of the Green’s function, stated as (3.6), the solution of (2.2a) and (3.2) can be expressed, in terms of the point sources $\{f_j\}_{j=1}^L$ (3.3), as

$$(3.11) \quad u_{x,y} = \sum_{j=1}^L \mathcal{G}_{|\mathbf{x}-j|,y} f_j, \quad (\mathbf{x}, \mathbf{y}) \in \mathbb{H}.$$

The solution (3.11) decays exponentially as $|\mathbf{x}|, |\mathbf{y}| \rightarrow \infty$ on \mathbb{H} under the assumption $\varepsilon > 0$. However, the definition (3.3) includes the scattered field $\{u_{x,0}\}_{x=1}^L$ on the perturbed sites. Indeed, by substituting (3.3) into (3.11), we find that $u_{x,y} = -m_s \omega^2 \sum_{j=1}^L \mathcal{G}_{|\mathbf{x}-j|,y} \mu_j (u_{j,0} + \widehat{\mathbf{u}}_{j,0})$, $(\mathbf{x}, \mathbf{y}) \in \mathbb{H}$, so that by restricting the solution u (3.11) to $\partial\mathbb{H}$, we have the discrete Lippmann–Schwinger equation

$$(3.12) \quad u_{x,0} = -m_s \omega^2 \sum_{j=1}^L \mathcal{G}_{|\mathbf{x}-j|,0} \mu_j (u_{j,0} + \widehat{\mathbf{u}}_{j,0}), \quad \mathbf{x} \in \mathbb{Z},$$

Downloaded 01/09/25 to 129.104.78.167 . Redistribution subject to SIAM license or copyright; see https://pubs.siam.org/terms-privacy

where according to (3.6)

$$(3.13) \quad \mathcal{G}_{|x|,0} = \frac{1}{2\pi i} \int_{\mathbb{T}} \frac{\mathfrak{z}^{|x|-1}}{\mathfrak{R}_s(\mathfrak{z})} d\mathfrak{z}.$$

The above equation (3.12) for $\mathbf{x} \in [1, L] \cap \mathbb{Z}$ yields a closed system of linear algebraic equations for $\{u_{\mathbf{x},0}\}_{\mathbf{x}=1}^L$ so that the problem is reduced to the inversion of an $L \times L$ matrix.

Remark 3.4. Consider the following Fourier transforms:

$$(3.14) \quad f(\mathfrak{z}) = \sum_{j=1}^L \mathfrak{z}^{-j} f_j, \quad u_0^F(\mathfrak{z}) = \sum_{\mathbf{x} \in \mathbb{Z}} u_{\mathbf{x},0} \mathfrak{z}^{-\mathbf{x}}, \quad \mathcal{G}_0^F(\mathfrak{z}) = \sum_{\mathbf{x} \in \mathbb{Z}} \mathcal{G}_{\mathbf{x},0} \mathfrak{z}^{-\mathbf{x}},$$

using (3.3) in the first expression and (3.13) in the third. Using (3.12) and the Fourier transforms $f, u_0^F, \mathcal{G}_0^F$ defined in (3.14), it follows that

$$(3.15) \quad \mathfrak{R}_s(\mathfrak{z}) u_0^F(\mathfrak{z}) = f(\mathfrak{z}),$$

as $\mathfrak{R}_s(\mathfrak{z}) \mathcal{G}_0^F(\mathfrak{z}) = 1$. Further, by Remark 3.2, \mathcal{G}_0^F satisfies the property

$$(3.16) \quad \mathcal{G}_0^F(\mathfrak{z}) = \mathcal{G}_0^F(\mathfrak{z}^{-1}).$$

Using the expression (3.13) for the Green's function evaluated on $\partial\mathbb{H}$, and the definition (3.3), the scattered field, as given by (3.12), on the perturbed sites can be concisely, but formally, solved to obtain

$$(3.17) \quad \mathbf{u} = (\mathbf{I} - \mathbf{T}\mathbf{D}(\boldsymbol{\mu}))^{-1} \mathbf{T}\mathbf{D}(\boldsymbol{\mu})\hat{\mathbf{u}},$$

where

$$(3.18a) \quad \mathbf{T} = \text{Toeplitz}(\mathcal{G}_{0,0}, \mathcal{G}_{1,0}, \mathcal{G}_{2,0}, \dots, \mathcal{G}_{L-1,0}) \in \mathbb{C}^{L \times L},$$

$$(3.18b) \quad \mathbf{D}(\boldsymbol{\mu}) = -m_s \omega^2 \text{diag}(\mu_1, \mu_2, \dots, \mu_L) \in \mathbb{C}^{L \times L},$$

$$(3.18c) \quad \mathbf{u} = (u_{1,0}, u_{2,0}, \dots, u_{L,0}) \in \mathbb{C}^L, \quad \hat{\mathbf{u}} = \hat{\mathfrak{a}} \mathfrak{z}_0(1, \mathfrak{z}_0, \mathfrak{z}_0^2, \dots, \mathfrak{z}_0^{L-1}) \in \mathbb{C}^L,$$

$$(3.18d) \quad \text{and } \mathbf{z} = \mathfrak{z}(1, \mathfrak{z}, \mathfrak{z}^2, \dots, \mathfrak{z}^{L-1}) \in \mathbb{C}^L.$$

Note that \mathbf{T} (3.18a) is a symmetric Toeplitz matrix due to the properties of Green's function as evident from (3.12) and (3.13). Using the above result (3.17) component-wise in (3.3), the complete solution for the scattered field on \mathbb{H} is given by (3.11).

3.1. Reflection and transmission coefficients for surface wave incidence.

For $\mathbf{x} \in \mathbb{Z}^-$, as $\varepsilon \rightarrow 0+$ and $\mathbf{x} \rightarrow -\infty$, according to (3.12),

$$(3.19) \quad u_{\mathbf{x},0} = -m_s \omega^2 \sum_{j=1}^L \mu_j \mathcal{G}_{-\mathbf{x}+j,0}(u_{j,0} + \hat{u}_{j,0}) = R \hat{\mathfrak{a}} \mathfrak{z}_0^{-\mathbf{x}}.$$

Hence, using the Cauchy residue theorem to evaluate (3.13) considering the fact that $\mathfrak{z}_0 < 1$ for $\varepsilon > 0$, the reflection coefficient is given by

$$(3.20) \quad \begin{aligned} R &= -\frac{m_s \omega^2}{\hat{\mathfrak{a}}} \left(\frac{1}{\mathfrak{z} \mathfrak{R}'_s(\mathfrak{z})} \right) \Big|_{\mathfrak{z}=\mathfrak{z}_0} \sum_{j=1}^L \mu_j \mathfrak{z}_0^j (u_{j,0} + \hat{u}_{j,0}) \\ &= \frac{1}{\hat{\mathfrak{a}}} \left(\frac{1}{\mathfrak{z} \mathfrak{R}'_s(\mathfrak{z})} \right) \Big|_{\mathfrak{z}=\mathfrak{z}_0} \mathfrak{z}_0(1, \mathfrak{z}_0, \mathfrak{z}_0^2, \dots, \mathfrak{z}_0^{L-1}) \cdot \mathbf{D}(\boldsymbol{\mu})(\mathbf{u} + \hat{\mathbf{u}}), \end{aligned}$$

where the second line uses (3.18c)₂. The factor $1/\hat{a}$ in (3.20) appears due to our, slightly general, choice of nonnormalized incident wave (3.1), but it eventually cancels with the contribution from the amplitude of the incident field and scattered field (by linearity) so that R is independent of \hat{a} .

For $\mathbf{x} > L$, as $\varepsilon \rightarrow 0+$, $\mathbf{x} \rightarrow +\infty$, $u_{\mathbf{x},0} = -m_s \omega^2 \sum_{j=1}^L \mu_j \mathcal{G}_{\mathbf{x}-j,0}(u_{j,0} + \hat{u}_{j,0})$, which in turn implies that the total field behaves as

$$(3.21) \quad u_{\mathbf{x},0} + \hat{u}_{\mathbf{x},0} = \hat{u}_{\mathbf{x},0} + (-m_s \omega^2) \sum_{j=1}^L \mu_j \mathcal{G}_{\mathbf{x}-j,0}(u_{j,0} + \hat{u}_{j,0}) = T \hat{a} \mathfrak{z}_0^{\mathbf{x}}.$$

Simplifying the expression in the same way as that of the reflection coefficient R (3.20), we find that the transmission coefficient is, therefore, given by

$$(3.22) \quad \begin{aligned} T &= 1 + \frac{(-m_s \omega^2)}{\hat{a}} \left(\frac{1}{\mathfrak{z} \mathfrak{K}'_s(\mathfrak{z})} \right) \Big|_{\mathfrak{z}=\mathfrak{z}_0} \sum_{j=1}^L \mu_j \mathfrak{z}_0^{-j} (u_{j,0} + \hat{u}_{j,0}) \\ &= 1 + \frac{1}{\hat{a}} \left(\frac{1}{\mathfrak{z} \mathfrak{K}'_s(\mathfrak{z})} \right) \Big|_{\mathfrak{z}=\mathfrak{z}_0} \mathfrak{z}_0^{-1} (1, \mathfrak{z}_0^{-1}, \mathfrak{z}_0^{-2}, \dots, \mathfrak{z}_0^{-L+1}) \cdot \mathbf{D}(\boldsymbol{\mu})(\mathbf{u} + \hat{\mathbf{u}}). \end{aligned}$$

With $\hat{\mathbf{u}} = \hat{a} \mathfrak{z}_0 (1, \mathfrak{z}_0, \mathfrak{z}_0^2, \dots, \mathfrak{z}_0^{L-1})$ as in (3.18c)₂, using (3.17), the reflection coefficient R (3.20) can be succinctly expressed as

$$(3.23) \quad R = \frac{1}{\hat{a}^2} \left(\frac{1}{\mathfrak{z} \mathfrak{K}'_s(\mathfrak{z})} \right) \Big|_{\mathfrak{z}=\mathfrak{z}_0} \mathbf{D}(\boldsymbol{\mu}) \hat{\mathbf{u}} \cdot (\mathbf{I} - \mathbf{T} \mathbf{D}(\boldsymbol{\mu}))^{-1} \hat{\mathbf{u}},$$

while the transmission coefficient T (3.22) is given by

$$(3.24) \quad T = 1 + \frac{1}{|\hat{a}|^2} \left(\frac{1}{\mathfrak{z} \mathfrak{K}'_s(\mathfrak{z})} \right) \Big|_{\mathfrak{z}=\mathfrak{z}_0} \mathbf{D}(\boldsymbol{\mu}) \widehat{\mathbf{u}} \cdot (\mathbf{I} - \mathbf{T} \mathbf{D}(\boldsymbol{\mu}))^{-1} \hat{\mathbf{u}}.$$

The expressions (3.23), (3.24) are utilized later in the article for numerical evaluations and graphical illustrations. At this point it is clear that, using the coefficients (3.20), (3.22), one can determine the energy flux in the surface waves reflected by the patch of size L of perturbed masses and transmitted across it. More importantly, what remains to be proven is the fact that all propagative waves, including waves excited in the bulk lattice, carry energy flux that equals that of the incident wave. This task is carried out next.

3.2. Energy conservation. The energy flux in the surface wave (2.3) is [7]

$$(3.25) \quad \begin{aligned} \mathcal{E}(k_0) &= \frac{1}{2} \omega^2 |u_{0,0}|^2 \mu_s(k_0) v_s(k_0), \\ \text{with } \mu_s(k_0) &:= (m_s - 1) + (1 - e^{-2\eta(k_0)})^{-1}, \end{aligned}$$

where v_s is defined as in (2.7). The effective mass μ_s satisfies $\mu_s(k_0) = \mu_s(-k_0)$ as $\eta(k_0) = \eta(-k_0)$ while $v_s(k_0) = -v_s(-k_0)$. Using the expression (3.25), the incident surface wave carries the energy flux [40]

$$(3.26) \quad \widehat{\mathcal{E}} = \mathcal{E}(k_0),$$

with $\hat{u}_{0,0} = \hat{a}$ replacing $u_{0,0}$. The expression of energy flux is obtained, as in Appendix 1 of [40], from the standard definition [7]

$$(3.27) \quad \widehat{\mathcal{E}} := \lim_{\mathbf{x} \rightarrow -\infty} \frac{1}{2} \operatorname{Re} \sum_{y \in \mathbb{Z} - \cup \{0\}} \hat{\mathbf{f}}_{\mathbf{x},y} \overline{\hat{\mathbf{u}}_{\mathbf{x},y}},$$

where $\widehat{\mathbf{f}}_{\mathbf{x},\mathbf{y}}$ denotes the force on particle at (\mathbf{x}, \mathbf{y}) from the interaction with $(\mathbf{x} - 1, \mathbf{y})$ while $\widehat{\mathbf{u}}_{\mathbf{x},\mathbf{y}}$ denotes the velocity of the particle at (\mathbf{x}, \mathbf{y}) ; indeed, $\widehat{\mathbf{u}}_{\mathbf{x},\mathbf{y}} = -i\omega\widehat{\mathbf{u}}_{\mathbf{x},\mathbf{y}}$. In view of Remark 3.1 and the statements regarding the recovery of scattered field via the absorption principle, it is noted that the limits $\mathbf{x} \rightarrow -\infty$ and $\varepsilon \rightarrow 0^+$, in (3.27), do not commute, and, in particular, the former is carried out after the latter. The expression (3.25), (3.26) can be simplified for the incident surface wave, as in (3.1) with amplitude $\widehat{\mathbf{a}}$, to the form

$$(3.28) \quad \widehat{\mathcal{E}} = \frac{1}{2} |\widehat{\mathbf{a}}|^2 \omega \frac{\sin k_0}{\rho(\gamma_0)},$$

where, using (3.8) and Remark 3.3,

$$(3.29) \quad \frac{1}{\rho(\gamma_0)} = \frac{\mathfrak{z}_0 \mathfrak{K}'_s(\mathfrak{z}_0)}{(\mathfrak{z}_0 - \mathfrak{z}_0^{-1})} = \frac{|\mathfrak{K}'_s(\mathfrak{z}_0)|}{2 \sin k_0}.$$

Under the assumption of point mass perturbation of finite size, we observe that the transmitted surface wave u^T has the same form as the incident wave $\widehat{\mathbf{u}}$ and the same wave number k_0 . Therefore, analogous to (3.27), the energy flux carried by the transmitted surface wave, with amplitude T , is

$$(3.30) \quad \mathcal{E}_T = \frac{1}{2} |\widehat{\mathbf{a}}|^2 |T|^2 \omega \frac{\sin k_0}{\rho(\gamma_0)}.$$

We also observe that the reflected surface wave u^R has the same form as the incident wave $\widehat{\mathbf{u}}$ but wave number $-k_0$; in the complex plane the corresponding point is \mathfrak{z}_0^{-1} and $u_{\mathbf{x},0}^R = \widehat{\mathbf{a}} R \mathfrak{z}_0^{-\mathbf{x}}$ (recall the discussion in the context of (3.20)). Thus, the energy flux in the reflected surface wave, with amplitude R , is given by

$$(3.31) \quad \mathcal{E}_R = \frac{1}{2} |\widehat{\mathbf{a}}|^2 |R|^2 \omega \frac{\sin k_0}{\rho(\gamma_0)}.$$

The energy leaked into the half space is

$$(3.32) \quad \mathcal{E}_{\mathbb{H}} = - \lim_{\mathbf{y} \rightarrow -\infty} \frac{1}{2} \operatorname{Re} \sum_{\mathbf{x} \in \mathbb{Z}} \mathbf{f}_{\mathbf{x},\mathbf{y}} \overline{\widehat{\mathbf{u}}_{\mathbf{x},\mathbf{y}}},$$

where $\mathbf{f}_{\mathbf{x},\mathbf{y}}$ denotes the force on particle at (\mathbf{x}, \mathbf{y}) from the interaction with $(\mathbf{x}, \mathbf{y} - 1)$ while taking into account the scattered wave field u on \mathbb{H} . With $\varepsilon \rightarrow 0^+$, using the Parseval theorem with the Fourier transforms (3.14), and the property (3.16), we find that the definition (3.32) leads to the expression

$$(3.33) \quad \mathcal{E}_{\mathbb{H}} = \frac{1}{2} \omega \frac{1}{2\pi i} \oint_{C_B} \operatorname{Im} \lambda(\mathfrak{z}) \frac{1}{2} (|u_0^F(\mathfrak{z})|^2 + |u_0^F(\mathfrak{z}^{-1})|^2) \mathfrak{z}^{-1} d\mathfrak{z},$$

since $|\lambda| = 1$ on C_B and $|\lambda| < 1$ outside C_B , where C_B is a counterclockwise contour almost coinciding with the branch cut for λ inside the unit circle. Note that the branch cut for λ coincides with the continuous spectrum (propagating and evanescent bulk waves) in the \mathfrak{z} plane. To obtain formula (3.33) from (3.32), assuming $\varepsilon > 0$, the contour \mathbb{T} in the associated contour integral similar to (3.13) is deformed into C_B taking into account the zeros of \mathfrak{K}_s in (3.7) (recall Remark 3.2 in this calculation). After this the limit $\varepsilon \rightarrow 0^+$ is taken and then the limit $\mathbf{y} \rightarrow -\infty$ in (3.32) is considered using the statement immediately preceding Remark 3.2. See Figure 2 for an exaggerated schematic of C_B assuming $\varepsilon > 0$.

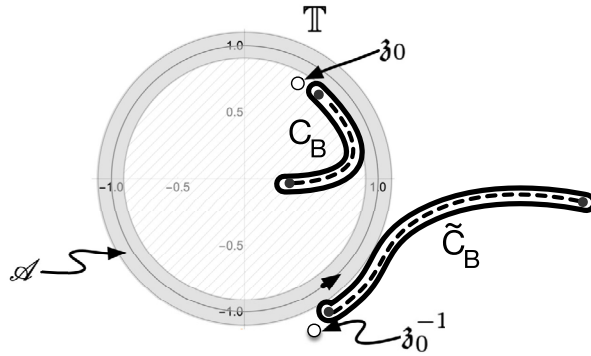


FIG. 2. Schematic of the counterclockwise contour C_B in the complex plane \mathbb{C} . \tilde{C}_B is related to C_B by the mapping $\mathfrak{z} \mapsto 1/\mathfrak{z}$. The thickness of gray annular region \mathcal{A} containing the unit circle depends on ε and shrinks as $\varepsilon \rightarrow 0+$.

PROPOSITION 3.5. We have the conservation of energy relation

$$(3.34) \quad \mathcal{E}_R + \mathcal{E}_T + \mathcal{E}_{\mathbb{H}} = \widehat{\mathcal{E}},$$

where $\widehat{\mathcal{E}}$ is given by (3.27), \mathcal{E}_R is given by (3.31), \mathcal{E}_T is given by (3.30), and $\mathcal{E}_{\mathbb{H}}$ is given by (3.33).

Proof. Recall Remark 3.4. Using (3.15), (3.14), (3.28), (3.30), (3.31), and (3.33), and (3.7), the statement of energy balance (3.34) becomes

$$(3.35) \quad \frac{1}{2}\omega \frac{1}{2\pi i} \oint_{C_B} \frac{\text{Im} \lambda_{\gamma} \frac{1}{2} (|f(\mathfrak{z})|^2 + |f(\mathfrak{z}^{-1})|^2)}{(\mathfrak{F}_s + \lambda)(\mathfrak{F}_s + \lambda^{-1})} \mathfrak{z}^{-1} d\mathfrak{z} + \frac{1}{2}\omega \frac{|f(\mathfrak{z}_0^{-1})|^2 + |f(\mathfrak{z}_0)|^2}{-2i\mathfrak{z}_0 \mathfrak{K}'_s(\mathfrak{z}_0)} + \frac{1}{2}\omega \text{Im} (f(\mathfrak{z}_0)) = 0.$$

The first two terms in (3.35) can be combined by an application of Cauchy’s residue theorem to rewrite (3.34) as

$$(3.36) \quad \frac{1}{2}\omega \frac{1}{2\pi i} \oint_{\mathbb{T}} \frac{\text{Im} \lambda_{\gamma} \frac{1}{2} (|f(\mathfrak{z})|^2 + |f(\mathfrak{z}^{-1})|^2)}{(\mathfrak{F}_s + \lambda)(\mathfrak{F}_s + \lambda^{-1})} \mathfrak{z}^{-1} d\mathfrak{z} + \frac{1}{2}\omega \text{Im} (f(\mathfrak{z}_0)) = 0.$$

Consider the expression $W := -\frac{1}{2} \text{Re} \sum_{x=1}^L f_x \overline{u_{x,0}}$ using (3.3). By an application of the Plancherel theorem

$$(3.37) \quad W = -\frac{1}{2}\omega \frac{1}{2\pi i} \oint_{\mathbb{T}} |f(\mathfrak{z})|^2 \frac{1}{2} \text{Im} \left(\frac{1}{\mathfrak{K}(\mathfrak{z})} + \frac{1}{\mathfrak{K}(\mathfrak{z}^{-1})} \right) \mathfrak{z}^{-1} d\mathfrak{z},$$

which upon using the definitions (3.7) leads to

$$(3.38) \quad W = \frac{1}{2}\omega \frac{1}{2\pi i} \oint_{\mathbb{T}} \frac{\text{Im} \lambda_{\gamma} \frac{1}{2} (|f(\mathfrak{z})|^2 + |f(\mathfrak{z}^{-1})|^2)}{(\mathfrak{F}_s + \lambda)(\mathfrak{F}_s + \lambda^{-1})} \mathfrak{z}^{-1} d\mathfrak{z}.$$

On the other hand, using (3.3) and by the direct substitution of expression of the incident wave, it is found that

$$(3.39) \quad W = -\frac{1}{2}\omega \text{Im} (f(\mathfrak{z}_0)).$$

The equations (3.38), (3.39) lead to (3.36). □

Remark 3.6. The statement of Proposition 3.5 can be equivalently expressed as

$$(3.40) \quad |R|^2 + |T|^2 + \mathcal{D} = 1,$$

where $\mathcal{D} = \mathcal{E}_{\mathbb{H}}/\mathcal{E} > 0$ is the energy flux radiated into the lattice half plane \mathbb{H} per unit incident wave energy flux while $|R|^2$ and $|T|^2$ represent the surface wave reflectance and transmittance, respectively.

4. Multiscale analysis for small, random mass perturbations. We assume again that ω belongs to the regime when a surface wave mode (2.3) can exist in the unperturbed lattice model, i.e., $\omega \in (0, \omega_{\max})$, where ω_{\max} is given by (2.6). We assume that there is a unit-amplitude forward-going (normalized) surface mode incoming from the left region $\mathbf{x} \leq 0$ and radiation condition into the right region $\mathbf{x} \geq L+1$ (the radiation condition expresses the fact that no left-going surface wave is incoming from the right region).

The total wave field \mathbf{u} is solution of (2.2a) for $y \neq 0$,

$$(4.1) \quad \alpha_s(\mathbf{u}_{\mathbf{x}+1,y} + \mathbf{u}_{\mathbf{x}-1,y} - 2\mathbf{u}_{\mathbf{x},y}) + \mathbf{u}_{\mathbf{x},y-1} - \mathbf{u}_{\mathbf{x},y} + m_s \omega^2 \mathbf{u}_{\mathbf{x},y} = 0, \quad y = 0,$$

for $\mathbf{x} \notin [1, L] \cap \mathbb{Z}$, and

$$(4.2) \quad \alpha_s(\mathbf{u}_{\mathbf{x}+1,y} + \mathbf{u}_{\mathbf{x}-1,y} - 2\mathbf{u}_{\mathbf{x},y}) + \mathbf{u}_{\mathbf{x},y-1} - \mathbf{u}_{\mathbf{x},y} + m_s(1 + \mu_x)\omega^2 \mathbf{u}_{\mathbf{x},y} = 0, \quad y = 0,$$

for $\mathbf{x} \in [1, L] \cap \mathbb{Z}$.

We denote by $\hat{\mathbf{u}}$ the propagative surface wave mode that is incident from the left side:

$$(4.3) \quad \hat{\mathbf{u}}_{\mathbf{x},y} = e^{ik(\gamma_0)\mathbf{x}} \phi_{\gamma_0}(y),$$

where $k(\gamma_0)$ is actually k_0 as previously stated in Remark 2.2; however we use the former to bring out the role of the function k (2.22). Note that the expression (4.3) coincides with that stated in (3.1) provided the amplitude is chosen such that $\hat{\mathbf{a}} = \sqrt{\rho(\gamma_0)}$.

We denote by $u = \mathbf{u} - \hat{\mathbf{u}}$, as in section 3, the scattered field that satisfies the following radiating conditions:

- (i) for $\gamma \in (0, \omega^2) \cup \{\gamma_0\}$, $\langle u_{\mathbf{x},\cdot}, \phi_\gamma \rangle \exp(ik(\gamma)\mathbf{x})$ does not depend on \mathbf{x} for $\mathbf{x} \leq 0$ and $\langle u_{\mathbf{x},\cdot}, \phi_\gamma \rangle \exp(-ik(\gamma)\mathbf{x})$ does not depend on \mathbf{x} for $\mathbf{x} \geq L+1$;
- (ii) for $\gamma \in (\omega^2 - 4, 0)$, $\langle u_{\mathbf{x},\cdot}, \phi_\gamma \rangle \exp(-k(\gamma)\mathbf{x})$ does not depend on \mathbf{x} for $\mathbf{x} \leq 0$ and $\langle u_{\mathbf{x},\cdot}, \phi_\gamma \rangle \exp(k(\gamma)\mathbf{x})$ does not depend on \mathbf{x} for $\mathbf{x} \geq L+1$.

We define by R the amplitude of the left-going surface mode in the left region $\mathbf{x} \leq 0$ and by T the amplitude of the right-going surface mode in the right region $\mathbf{x} \geq L+1$:

$$(4.4) \quad R = \langle u_{\mathbf{x},\cdot}, \phi_{\gamma_0} \rangle \exp(ik(\gamma_0)\mathbf{x}) \text{ for } \mathbf{x} \leq 0,$$

$$(4.5) \quad T = \langle u_{\mathbf{x},\cdot}, \phi_{\gamma_0} \rangle \exp(-ik(\gamma_0)\mathbf{x}) \text{ for } \mathbf{x} \geq L+1.$$

We refer to R , respectively, T , as the reflection, respectively, transmission, coefficient, as in section 3.

The total wave field \mathbf{u} can be expanded as (2.17). The modal amplitudes $\check{\mathbf{u}}_\gamma(\mathbf{x}) = \langle u_{\mathbf{x},\cdot}, \phi_\gamma \rangle$ satisfy the coupled difference equations

$$(4.6) \quad \begin{aligned} & \check{\mathbf{u}}_\gamma(\mathbf{x} + 1) + \check{\mathbf{u}}_\gamma(\mathbf{x} - 1) + (\gamma - 2)\check{\mathbf{u}}_\gamma(\mathbf{x}) = -m_s \mu_x \omega^2 \sqrt{\rho(\gamma)} \\ & \times \left[\sqrt{\rho(\gamma_0)} \check{\mathbf{u}}_{\gamma_0}(\mathbf{x}) + \int_{\omega^2-4}^{\omega^2} \sqrt{\rho(v)} \check{\mathbf{u}}_v(\mathbf{x}) dv \right], \quad \mathbf{x} \in [1, L]. \end{aligned}$$

4.1. Moments of the reflectance, transmittance, and radiative loss. We assume that the $(\mu_x)_{x \in [1, L] \cap \mathbb{Z}}$ are independent and identically distributed random variables with mean zero and variance σ^2 . We address the regime where the fluctuations of the lattice parameters within the perturbed region are small but the perturbed region is large, so that the effect of the perturbations will be of order one. Accordingly, we here carry out a multiscale analysis in the asymptotic framework $\sigma \ll 1$ and $L \gg 1$ such that $L\sigma^2 = O(1)$. We prove, in section 5, the following proposition, which is the main result of the paper.

PROPOSITION 4.1. *Let us denote*

$$(4.7) \quad \frac{1}{L_{\text{loc}}} = \frac{\sigma^2 m_s^2 \omega^4 \rho(\gamma_0)^2}{4 \sin^2(k(\gamma_0))}, \quad \Lambda = \frac{\sigma^2 m_s^2 \omega^4 \rho(\gamma_0)}{2 \sin k(\gamma_0)} \int_0^{\omega^2} \frac{\rho(\gamma)}{\sin k(\gamma)} d\gamma.$$

We denote by $\mathcal{R}_p^\sigma(\tilde{L}) = \mathbb{E}[|R(L = [\tilde{L} L_{\text{loc}}])|^{2p}]$, $p \geq 0$, the moments of the reflection coefficient for $L = [\tilde{L} L_{\text{loc}}]$ (which is of the order of σ^{-2} when \tilde{L} is of order one).

In the limit $\sigma \rightarrow 0$, the moments of the reflection coefficient $(\mathcal{R}_p^\sigma)_{p \geq 0}$ converge to the solution $(\mathcal{R}_p)_{p \geq 0}$ of the system

$$(4.8) \quad \partial_{\tilde{L}} \mathcal{R}_p = p^2 (\mathcal{R}_{p+1} + \mathcal{R}_{p-1} - 2\mathcal{R}_p) - 2\tilde{\Lambda} p \mathcal{R}_p,$$

starting from $\mathcal{R}_p(\tilde{L} = 0) = \mathbf{1}_0(p)$, where

$$(4.9) \quad \tilde{\Lambda} = \Lambda L_{\text{loc}} = 2 \frac{\sin k(\gamma_0)}{\rho(\gamma_0)} \int_0^{\omega^2} \frac{\rho(\gamma)}{\sin k(\gamma)} d\gamma.$$

Similarly, we find that $(\mathbb{E}[|R|^{2p}|T|^2])_{p \geq 0}$ converges to the solution $(\mathcal{T}_p)_{p \geq 0}$ of the system

$$(4.10) \quad \partial_{\tilde{L}} \mathcal{T}_p = ((p+1)^2 (\mathcal{T}_{p+1} - \mathcal{T}_p) + p^2 (\mathcal{T}_{p-1} - \mathcal{T}_p)) - \tilde{\Lambda} (2p+1) \mathcal{T}_p,$$

starting from $\mathcal{T}_p(\tilde{L} = 0) = \mathbf{1}_0(p)$, and $(\mathbb{E}[|R|^{2p}|T|^4])_{p \geq 0}$ converges to the solution $(\mathcal{U}_p)_{p \geq 0}$ of the system

$$(4.11) \quad \partial_{\tilde{L}} \mathcal{U}_p = ((p+2)^2 (\mathcal{U}_{p+1} - \mathcal{U}_p) + p^2 (\mathcal{U}_{p-1} - \mathcal{U}_p)) + (2 - \tilde{\Lambda} (2p+2)) \mathcal{U}_p,$$

starting from $\mathcal{U}_p(\tilde{L} = 0) = \mathbf{1}_0(p)$,

Following [14, section 9.2.2], the solutions of these systems have probabilistic representations (see Appendix B for a brief introduction to jump Markov processes). In particular,

$$(4.12) \quad \mathcal{R}_p(\tilde{L}) = \mathbb{E} \left[\mathbf{1}_{N_{\tilde{L}}^R = 0} \exp \left(-2\tilde{\Lambda} \int_0^{\tilde{L}} N_x^R dx \right) \mid N_0^R = p \right], \quad p \geq 0,$$

where $(N_x^R)_{x \geq 0}$ is a jump Markov process with state space \mathbb{N} and with generator $\mathcal{L}^R f(n) = n^2(f(n+1) + f(n-1) - 2f(n))$. This expression for $p = 1$ gives the expectation of $|R|^2$, and the expressions for $p = 1$ and $p = 2$ give the variance of $|R|^2$ in the limit $\sigma \rightarrow 0$. Similarly,

$$(4.13) \quad \mathcal{T}_p(\tilde{L}) = \mathbb{E} \left[\mathbf{1}_{N_{\tilde{L}}^T = 0} \exp \left(-\tilde{\Lambda} \int_0^{\tilde{L}} 2N_x^T + 1 dx \right) \mid N_0^T = p \right], \quad p \geq 0,$$

where $(N_x^T)_{x \geq 0}$ is a jump Markov process with state space \mathbb{N} and with generator $\mathcal{L}^T f(n) = (n+1)^2(f(n+1) - f(n)) + n^2(f(n-1) - f(n))$. This expression for $p=0$ gives the expectation of $|T|^2$ in the limit $\sigma \rightarrow 0$. We also have

$$(4.14) \quad \mathcal{U}_p(\tilde{L}) = \exp(2\tilde{L}) \mathbb{E} \left[\mathbf{1}_{N_{\tilde{L}}^U=0} \exp \left(-\tilde{\Lambda} \int_0^{\tilde{L}} 2N_x^U + 2dx \right) \mid N_0^U = p \right], \quad p \geq 0,$$

where $(N_x^U)_{x \geq 0}$ is a jump Markov process with state space \mathbb{N} and with generator $\mathcal{L}^U f(n) = (n+2)^2(f(n+1) - f(n)) + n^2(f(n-1) - f(n))$. This expression for $p=0$ gives the second moment of $|T|^2$, which in turn gives the variance of $|T|^2$ in the limit $\sigma \rightarrow 0$. These results can also be exploited to determine the moments of the radiative loss. Indeed, using the energy conservation relation (3.40) $\mathcal{D} + |R|^2 + |T|^2 = 1$, the mean radiative loss is

$$(4.15) \quad \mathbb{E}[\mathcal{D}] = 1 - \mathbb{E}[|R|^2] - \mathbb{E}[|T|^2],$$

and its variance is

$$(4.16) \quad \text{Var}(\mathcal{D}) = \mathbb{E}[|R|^4] + 2\mathbb{E}[|R|^2|T|^2] + \mathbb{E}[|T|^4] - \mathbb{E}[|R|^2]^2 - 2\mathbb{E}[|R|^2]\mathbb{E}[|T|^2] - \mathbb{E}[|T|^2]^2.$$

4.2. Closed form expressions for two regimes. It seems that it is not possible to find closed form expressions for $\mathcal{R}_1(\tilde{L})$ and $\mathcal{T}_1(\tilde{L})$, which means that we cannot give closed form expressions for $\mathbb{E}[|R|^2]$ and $\mathbb{E}[|T|^2]$ when $\mathbf{L} = [\tilde{L} \mathbf{L}_{\text{loc}}]$ in the limit $\sigma \rightarrow 0$. However, we can find closed form expressions for the Taylor series expansions of $\mathcal{R}_1(\tilde{L})$ and $\mathcal{T}_1(\tilde{L})$ when $\tilde{L} \ll 1$. This means that we can give approximate expressions for $\mathbb{E}[|R|^2]$ and $\mathbb{E}[|T|^2]$ when $\mathbf{L} = [\tilde{L} \mathbf{L}_{\text{loc}}]$ in the limit $\sigma \rightarrow 0$ that are valid up to a relative error equal to \tilde{L} (or even \tilde{L}^2 if one takes the second-order series expansions). The regime $\tilde{L} \ll 1$ is called the weakly scattering regime, because $\mathbb{E}[|T|^2] \simeq 1$ as we will see below. A similar statement is true when $\tilde{L} \gg 1$ and this regime is called the strongly scattering regime, because $\mathbb{E}[|T|^2] \simeq 0$.

(1) When $\tilde{L} \ll 1$, we can expand (4.12) and (4.13) to get (in the limit $\sigma \rightarrow 0$)

$$(4.17) \quad \mathbb{E}[|R|^2] = \tilde{L} - (1 + \tilde{\Lambda})\tilde{L}^2 + O(\tilde{L}^3),$$

$$(4.18) \quad \mathbb{E}[|T|^2] = 1 - (1 + \tilde{\Lambda})\tilde{L} + \left(1 + \tilde{\Lambda} + \frac{1}{2}\tilde{\Lambda}^2\right)\tilde{L}^2 + O(\tilde{L}^3),$$

$$(4.19) \quad \mathbb{E}[|R|^4] = 2\tilde{L}^2 + O(\tilde{L}^3),$$

$$(4.20) \quad \mathbb{E}[|T|^4] = 1 - 2(1 + \tilde{\Lambda})\tilde{L} + (4 + 4\tilde{\Lambda} + 2\tilde{\Lambda}^2)\tilde{L}^2 + O(\tilde{L}^3),$$

$$(4.21) \quad \mathbb{E}[|R|^2|T|^2] = \tilde{L} - (3 + 2\tilde{\Lambda})\tilde{L} + O(\tilde{L}^3),$$

and hence

$$(4.22) \quad \mathbb{E}[\mathcal{D}] = \tilde{\Lambda}\tilde{L} - \frac{1}{2}\tilde{\Lambda}^2\tilde{L}^2 + O(\tilde{L}^3) = \tilde{\Lambda}\tilde{L} + O(\tilde{L}^2),$$

$$(4.23) \quad \text{Var}(\mathcal{D}) = \tilde{L}^2 + O(\tilde{L}^3) = O(\tilde{L}^2).$$

In particular, we observe that the mean radiative loss is proportional to Λ to leading order:

$$(4.24) \quad \mathbb{E}[\mathcal{D}] \simeq \tilde{\Lambda}\tilde{L} = \Lambda \mathbf{L},$$

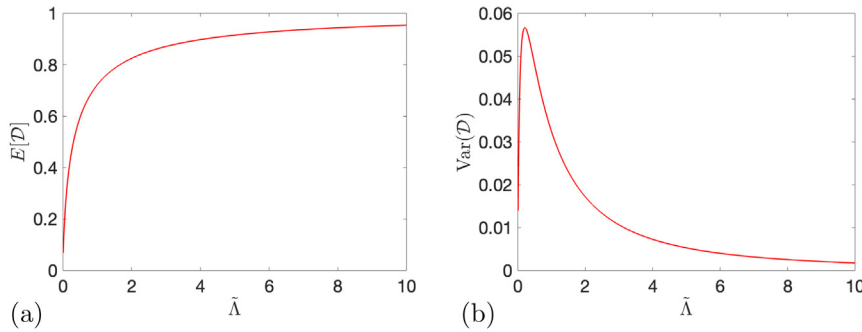


FIG. 3. (a) Mean (4.29) and (b) variance (4.30) of the radiative loss \mathcal{D} as functions of $\tilde{\Lambda}$ in the strongly scattering regime $\tilde{L} \gg 1$.

and the relative variance of radiative loss is constant:

$$(4.25) \quad \text{Var}(\mathcal{D})/\mathbb{E}[\mathcal{D}]^2 \simeq 1/\tilde{\Lambda}^2.$$

(2) When $\tilde{L} \gg 1$, proceeding as in [14, section 9.2.3], we find $\mathbb{E}[|T|^2] = 0$ and

$$(4.26) \quad \mathbb{E}[|R|^2] = 1 - 2\tilde{\Lambda} \exp(2\tilde{\Lambda}) E_1(2\tilde{\Lambda}),$$

where

$$(4.27) \quad E_1(x) := \int_1^\infty \frac{\exp(-xt)}{t} dt$$

and we remark that $\tilde{\Lambda}$ does not depend on σ . More generally, when $\tilde{L} \gg 1$, we have $\mathbb{E}[|T|^{2q}|R|^{2p}] = 0$ if $q \geq 1$ and

$$(4.28) \quad \mathbb{E}[|R|^{2p}] = \tilde{\Lambda} \int_0^\infty \left(\frac{s}{2+s}\right)^p \exp(-\tilde{\Lambda}s) ds$$

for any integer p . In particular, we observe that the mean radiative loss is a monotonically increasing function of $\tilde{\Lambda}$:

$$(4.29) \quad \mathbb{E}[\mathcal{D}] = 2\tilde{\Lambda} \exp(2\tilde{\Lambda}) E_1(2\tilde{\Lambda}),$$

where E_1 is defined as in (4.27), and the variance of the radiative loss is a function of $\tilde{\Lambda}$ as well (see Figure 3):

$$(4.30) \quad \text{Var}(\mathcal{D}) = [1 - 2\tilde{\Lambda} \exp(2\tilde{\Lambda}) E_1(2\tilde{\Lambda})] [1 + 2\tilde{\Lambda} + 2\tilde{\Lambda} \exp(2\tilde{\Lambda}) E_1(2\tilde{\Lambda})] - 1.$$

4.3. Comparison of ensemble of exact solutions versus asymptotics.

In the right of Figure 4(a), we compare the empirical averages of numerical simulations (for many different realizations of the random mass perturbations) in the left part of Figure 4(a) with the theoretical predictions for the expectation $\mathbb{E}[|T|^2]$ and the standard deviation $\text{Std}(|T|^2) = \text{Var}(|T|^2)^{1/2}$. The numerical simulations are based on the exact solution (3.24) and the theoretical predictions are based on (4.13) and (4.14). In a similar manner, in Figures 4(b) and 4(c), we compare the empirical averages of numerical simulations with the theoretical predictions for the expectation $\mathbb{E}[|R|^2]$, $\mathbb{E}[|R|^2 + |T|^2]$, and the standard deviation $\text{Std}(|R|^2)$. We again obtain an excellent

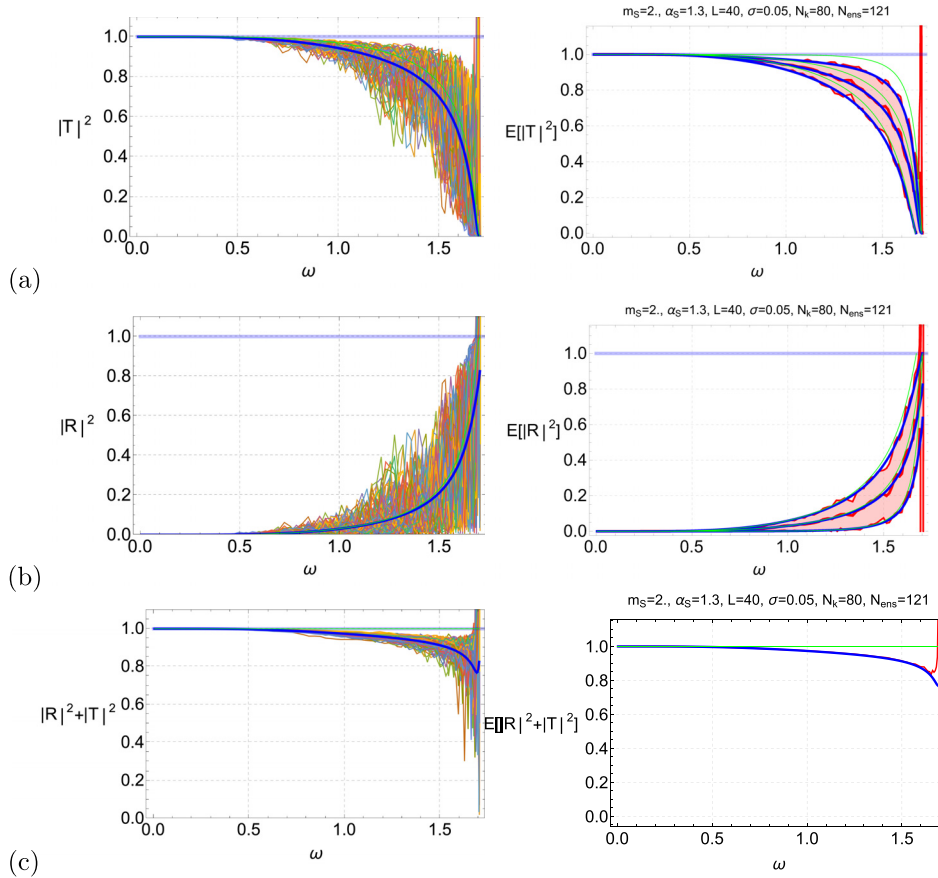


FIG. 4. Left: Realizations of (a) $|T|^2$, (b) $|R|^2$, (c) $|R|^2 + |T|^2$ using Green's function based exact solution (3.24) and independent and identically distributed mass perturbations. Right: Expectations and standard deviations of (a) $|T|^2$, (b) $|R|^2$, (c) $|R|^2 + |T|^2$. Blue curves are asymptotic formulas (4.12), (4.13). Red curves are empirical averages using (3.24). Green curves represent the theoretical results (4.31) when $\Lambda = 0$ (no coupling with radiative modes). The surface structure parameters m_s, α_s are assumed to be constant outside the perturbed patch $[1, L]$. Here $m_s = 2, \alpha_s = 1.3, L = 40, \sigma = 0.05$. (Color available online.)

agreement. We can observe that the behavior of the transmittance close to the right endpoint ω_{\max} (given by (2.6)) of the propagative band exhibits large deviations from the perfect transmission. The transmittance goes to one as $\omega \rightarrow 0$ and to zero as $\omega \rightarrow \omega_{\max}$. The numerical calculations of the exact solution for R and T for ω very close to ω_{\max} suffer from small errors associated with the evaluation of contour integral and vanishing of group velocity of the surface wave; this can be rectified by employing refined techniques, but we did not pursue that as it is a very narrow regime, and our focus remains on asymptotic results. Finally, the green curves in Figure 4 are the—wrong—predictions obtained by a theoretical analysis that would neglect the radiative modes. In such a case we have $|R|^2 + |T|^2 = 1$ and [14, section 7.1.5]

$$(4.31) \quad \mathbb{E}[|T|^2] |_{\Lambda=0} = \exp\left(-\frac{L}{L_{\text{loc}}}\right) \int_0^\infty \exp\left(-s^2 \frac{L}{L_{\text{loc}}}\right) \frac{2\pi s \sinh(\pi s)}{\cosh^2(\pi s)} ds.$$

As seen in Figures 4(a)–(b) both the reflectance and transmittance are significantly overestimated by this wrong approach. It is, therefore, of utmost importance to take

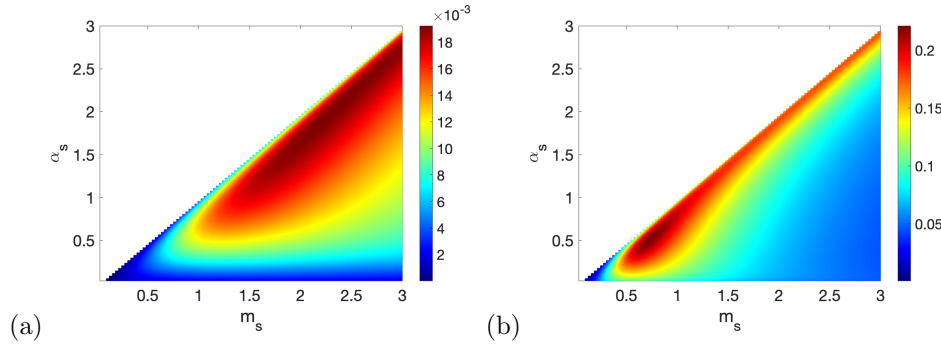


FIG. 5. Mean radiative loss $\mathbb{E}[\mathcal{L}] = 1 - \mathbb{E}[|R|^2 + |T|^2]$ at frequency (a) $\omega = 0.5\omega_{\max}$ and (b) $\omega = 0.9\omega_{\max}$, as a function of surface structure parameters m_s and α_s . For these plots, $\sigma = 0.05$, $L = 40$, and we use (4.12) and (4.13).

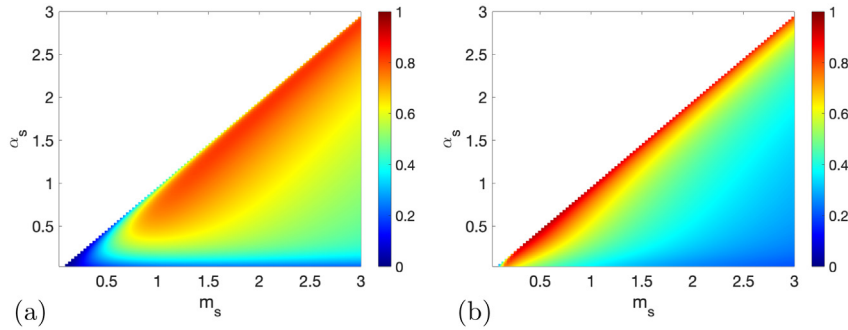


FIG. 6. Mean radiative loss $\mathbb{E}[\mathcal{L}] = 1 - \mathbb{E}[|R|^2 + |T|^2]$ at frequency (a) $\omega = 0.5\omega_{\max}$ and (b) $\omega = 0.9\omega_{\max}$, as a function of surface structure parameters m_s and α_s . For these plots, $\sigma = 0.05$, $L = 5000$, and we use (4.12) and (4.13).

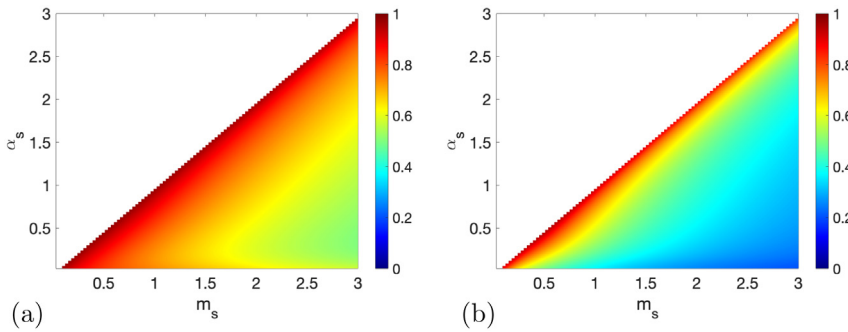


FIG. 7. Mean radiative loss $\mathbb{E}[\mathcal{L}] = 1 - \mathbb{E}[|R|^2 + |T|^2]$ at frequency (a) $\omega = 0.5\omega_{\max}$ and (b) $\omega = 0.9\omega_{\max}$, as a function of surface structure parameters m_s and α_s . For these plots, $L \rightarrow \infty$, and we use (4.29).

into account the coupling between surface and radiative modes, which can result in a significant amount of radiative loss.

4.4. Radiative loss: Dependence on surface structure. In Figures 5–7 we plot the mean radiative loss evaluated at $\omega = 0.5\omega_{\max}$ (left) and $\omega = 0.9\omega_{\max}$ (right) as functions of the surface structure parameters m_s and α_s (recall that ω_{\max} is given

by (2.6)). We can observe that the radiative loss becomes close to one in the strongly scattering regime and when m_s and α_s are close to each other. Indeed, when m_s and α_s are close to each other, the discrete eigenvalue of the operator (2.13) is close to the continuous spectrum, or equivalently, the wavenumber of the surface mode is close to the wavenumber interval of the radiative modes. Under such circumstances, the coupling between the surface mode and the radiative modes induced by the mass perturbations is strong, which explains the value close to one of the radiative loss.

5. Proof (multiscale analysis).

5.1. Modal expansion of the solution of the perturbed equation of motion. We introduce the generalized forward-going (right-going) and backward-going (left-going) mode amplitudes,

$$(5.1) \quad \{a_{\gamma_0}(\mathbf{x}), b_{\gamma_0}(\mathbf{x})\} \text{ and } \{a_\gamma(\mathbf{x}), b_\gamma(\mathbf{x}), \gamma \in (\omega^2 - 4, \omega^2)\},$$

which are defined by

$$(5.2) \quad a_\gamma(\mathbf{x}) = \frac{e^{-ik(\gamma)\mathbf{x}}}{2i\sqrt{\sin k(\gamma)}} \left(\check{u}_\gamma(\mathbf{x} + 1) - e^{-ik(\gamma)} \check{u}_\gamma(\mathbf{x}) \right),$$

$$(5.3) \quad b_\gamma(\mathbf{x}) = \frac{e^{ik(\gamma)\mathbf{x}}}{2i\sqrt{\sin k(\gamma)}} \left(-\check{u}_\gamma(\mathbf{x} + 1) + e^{ik(\gamma)} \check{u}_\gamma(\mathbf{x}) \right),$$

and which are such that

$$(5.4) \quad \frac{1}{\sqrt{\sin k(\gamma)}} (a_\gamma(\mathbf{x})e^{ik(\gamma)\mathbf{x}} + b_\gamma(\mathbf{x})e^{-ik(\gamma)\mathbf{x}}) = \check{u}_\gamma(\mathbf{x}),$$

$$(5.5) \quad (a_\gamma(\mathbf{x}) - a_\gamma(\mathbf{x} - 1))e^{ik(\gamma)\mathbf{x}} + (b_\gamma(\mathbf{x}) - b_\gamma(\mathbf{x} - 1))e^{-ik(\gamma)\mathbf{x}} = 0,$$

and

$$(5.6) \quad \begin{aligned} \check{u}_\gamma(\mathbf{x} + 1) + \check{u}_\gamma(\mathbf{x} - 1) + (\gamma - 2)\check{u}_\gamma(\mathbf{x}) &= -2i\sqrt{\sin k(\gamma)}e^{ik(\gamma)\mathbf{x}}(a_\gamma(\mathbf{x} - 1) - a_\gamma(\mathbf{x})) \\ &= 2i\sqrt{\sin k(\gamma)}e^{-ik(\gamma)\mathbf{x}}(b_\gamma(\mathbf{x} - 1) - b_\gamma(\mathbf{x})). \end{aligned}$$

From (4.6) we obtain the coupled system of random difference equations satisfied by the mode amplitudes in (5.1) for $\gamma \in (\omega^2 - 4, \omega^2) \cup \{\gamma_0\}$,

$$(5.7) \quad \begin{aligned} &a_\gamma(\mathbf{x} - 1) - a_\gamma(\mathbf{x}) \\ &= -\frac{im_s\omega^2\sqrt{\rho(\gamma)\rho(\gamma_0)}}{2\sqrt{\sin k(\gamma)\sin k(\gamma_0)}}\mu_{\mathbf{x}} \left[a_{\gamma_0}(\mathbf{x})e^{i(k(\gamma_0)-k(\gamma))\mathbf{x}} + b_{\gamma_0}(\mathbf{x})e^{i(-k(\gamma_0)-k(\gamma))\mathbf{x}} \right] \\ &\quad - \frac{im_s\omega^2\sqrt{\rho(\gamma)}}{2\sqrt{\sin k(\gamma)}}\mu_{\mathbf{x}} \int_0^{\omega^2} \frac{\sqrt{\rho(v)}}{\sqrt{\sin k(v)}} \left[a_v(\mathbf{x})e^{i(k(v)-k(\gamma))\mathbf{x}} + b_v(\mathbf{x})e^{i(-k(v)-k(\gamma))\mathbf{x}} \right] dv \\ &= -\frac{im_s\omega^2\sqrt{\rho(\gamma)}}{2\sqrt{\sin k(\gamma)}}\mu_{\mathbf{x}} \int_{\omega^2-4}^0 \sqrt{\rho(v)}\check{u}_v(\mathbf{x})e^{-ik(\gamma)\mathbf{x}}dv, \end{aligned}$$

$$\begin{aligned}
 & b_\gamma(\mathbf{x} - 1) - b_\gamma(\mathbf{x}) \\
 &= \frac{im_s \omega^2 \sqrt{\rho(\gamma)\rho(\gamma_0)}}{2\sqrt{\sin k(\gamma)\sin k(\gamma_0)}} \mu_{\mathbf{x}} \left[a_{\gamma_0}(\mathbf{x}) e^{i(k(\gamma_0)+k(\gamma))\mathbf{x}} + b_{\gamma_0}(\mathbf{x}) e^{i(-k(\gamma_0)+k(\gamma))\mathbf{x}} \right] \\
 &+ \frac{im_s \omega^2 \sqrt{\rho(\gamma)}}{2\sqrt{\sin k(\gamma)}} \mu_{\mathbf{x}} \int_0^{\omega^2} \frac{\sqrt{\rho(v)}}{\sqrt{\sin k(v)}} \left[a_v(\mathbf{x}) e^{i(k(v)+k(\gamma))\mathbf{x}} + b_v(\mathbf{x}) e^{i(-k(v)+k(\gamma))\mathbf{x}} \right] dv \\
 (5.8) \quad &+ \frac{im_s \omega^2 \sqrt{\rho(\gamma)}}{2\sqrt{\sin k(\gamma)}} \mu_{\mathbf{x}} \int_{\omega^2-4}^0 \sqrt{\rho(v)} \check{u}_v(\mathbf{x}) e^{ik(\gamma)\mathbf{x}} dv.
 \end{aligned}$$

This system is supplemented with boundary conditions corresponding to a unit-amplitude forward-going surface mode incoming from the left region $\mathbf{x} \leq 0$ and radiation conditions into the right region $\mathbf{x} \geq L+1$:

$$(5.9) \quad b_\gamma(L+1) = 0, \quad a_\gamma(0) = \mathbf{1}_{\gamma_0}(\gamma).$$

5.1.1. Role of the evanescent modes. The coupling with the evanescent modes can be captured by substituting the expression of the evanescent modes into the last terms of (5.7) and (5.8): for $\gamma \in (\omega^2 - 4, 0)$,

$$\check{u}_\gamma(\mathbf{x}) = - \sum_y \mu_y m_s \omega^2 \sqrt{\rho(\gamma)} \left[\sqrt{\rho(\gamma_0)} \check{u}_{\gamma_0}(\mathbf{y}) + \int_{\omega^2-4}^{\omega^2} \sqrt{\rho(v)} \check{u}_v(\mathbf{y}) dv \right] G_\gamma(\mathbf{x} - \mathbf{y}),$$

where $G_\gamma(\mathbf{x})$ is the radiating solution of

$$G_\gamma(\mathbf{x} + 1) + G_\gamma(\mathbf{x} - 1) + (\gamma - 2)G_\gamma(\mathbf{x}) = \mathbf{1}_0(\mathbf{x}),$$

that is to say,

$$\begin{aligned}
 (5.10) \quad G_\gamma(\mathbf{x}) &= g_\gamma \mathbf{1}_0(\mathbf{x}) + h_\gamma e^{-k(\gamma)|\mathbf{x}|} (1 - \mathbf{1}_0(\mathbf{x})), \\
 g_\gamma &= \frac{1 + e^{k(\gamma)}(\gamma - 2)}{\gamma - 2 + (\gamma^2 - 4\gamma + 2)e^{k(\gamma)}}, \\
 h_\gamma &= - \frac{e^{2k(\gamma)}}{\gamma - 2 + (\gamma^2 - 4\gamma + 2)e^{k(\gamma)}}
 \end{aligned}$$

for $\gamma \in (\omega^2 - 4, 0)$. The coupling with evanescent modes gives rise to an effective dispersion (i.e., a frequency-dependent phase modulation) as we will see below.

5.1.2. Diffusion approximation. It is not possible to directly apply diffusion approximation theory to the system (5.7)–(5.8) with boundary conditions (because the solution is not adapted to the filtration of the driving process μ , in the sense that the solution depends on $(\mu_{\mathbf{x}})_{\mathbf{x} \in [1, L]}$). The strategy is to apply diffusion approximation theory to the system (5.7)–(5.8) with initial conditions and to use the linearity of the system to deduce the behavior of the solution of the system with boundary conditions.

We first study the system (5.7)–(5.8) supplemented with initial conditions at $\mathbf{x} = 0$ instead of (5.9), and we denote such a solution by $(a_\gamma^{(i)}(\mathbf{x}), b_\gamma^{(i)}(\mathbf{x}))$. We apply the diffusion approximation theory set forth in [14], as in [10, Appendix B]. If $L = \lfloor L/\sigma^2 \rfloor$ and $\sigma^2 \rightarrow 0$, then $(a_{\gamma_0}^{(i)}(\lfloor x/\sigma^2 \rfloor), b_{\gamma_0}^{(i)}(\lfloor x/\sigma^2 \rfloor))_{x \in [0, L]}$ converges to the solution $(\mathbf{a}_{\gamma_0}^{(i)}(x), \mathbf{b}_{\gamma_0}^{(i)}(x))_{x \in [0, L]}$ of the diffusion equation

$$(5.11) \quad d \begin{pmatrix} \mathbf{a}_{\gamma_0}^{(i)}(x) \\ \mathbf{b}_{\gamma_0}^{(i)}(x) \end{pmatrix} = \frac{1}{\sqrt{L_{\text{loc}}}} \left\{ \begin{pmatrix} i & 0 \\ 0 & -i \end{pmatrix} \begin{pmatrix} \mathbf{a}_{\gamma_0}^{(i)}(x) \\ \mathbf{b}_{\gamma_0}^{(i)}(x) \end{pmatrix} dW_0(x) - \frac{1}{\sqrt{2}} \begin{pmatrix} 0 & 1 \\ 1 & 0 \end{pmatrix} \begin{pmatrix} \mathbf{a}_{\gamma_0}^{(i)}(x) \\ \mathbf{b}_{\gamma_0}^{(i)}(x) \end{pmatrix} dW_1(x) \right. \\ \left. + \frac{1}{\sqrt{2}} \begin{pmatrix} 0 & -i \\ i & 0 \end{pmatrix} \begin{pmatrix} \mathbf{a}_{\gamma_0}^{(i)}(x) \\ \mathbf{b}_{\gamma_0}^{(i)}(x) \end{pmatrix} dW_2(x) \right\} + \frac{\lambda + i\kappa}{2} \begin{pmatrix} -1 & 0 \\ 0 & 1 \end{pmatrix} \begin{pmatrix} \mathbf{a}_{\gamma_0}^{(i)}(x) \\ \mathbf{b}_{\gamma_0}^{(i)}(x) \end{pmatrix} dx,$$

with the prescribed initial conditions and with

$$(5.12) \quad \frac{1}{L_{\text{loc}}} = \frac{1}{\sigma^2 L_{\text{loc}}} = \frac{m_s^2 \omega^4 \rho(\gamma_0)^2}{4 \sin^2(k(\gamma_0))},$$

$$(5.13) \quad \kappa = \frac{m_s^2 \omega^4 \rho(\gamma_0)}{\sin k(\gamma_0)} \int_{\omega^2-4}^0 \rho(v) g_v dv,$$

$$(5.14) \quad \lambda = \frac{\Lambda}{\sigma^2} = \frac{m_s^2 \omega^4 \rho(\gamma_0)}{\sin k(\gamma_0)} \int_0^{\omega^2} \rho(v) g_v dv.$$

Here W_0, W_1, W_2 are independent standard Brownian motions and g_γ is defined by

$$(5.15) \quad g_\gamma = i \frac{1 + e^{-ik(\gamma)}(\gamma - 2)}{\gamma - 2 + (\gamma^2 - 4\gamma + 2)e^{-ik(\gamma)}} \\ = \frac{1}{\sqrt{(4 - \gamma)\gamma}} = \frac{1}{2 \sin k(\gamma)} \quad \text{for } \gamma \in (0, \omega^2),$$

which is real, positive valued. We can see that the coupling with the evanescent modes induces an effective dispersion term proportional to κ and the coupling with the radiative modes induces an effective diffusion term proportional to λ . We also remark that σ^2 does not appear in the expression of L_{loc}, κ , and λ , but remember that $L = [L/\sigma^2]$ and $(\mathbf{a}_{\gamma_0}^{(i)}(x), \mathbf{b}_{\gamma_0}^{(i)}(x))$ is the limit of $(a_{\gamma_0}^{(i)}([x/\sigma^2]), b_{\gamma_0}^{(i)}([x/\sigma^2]))$ as $\sigma \rightarrow 0$ so that $(a_{\gamma_0}^{(i)}(\mathbf{x}), b_{\gamma_0}^{(i)}(\mathbf{x})) \simeq (\mathbf{a}_{\gamma_0}^{(i)}(\sigma^2 \mathbf{x}), \mathbf{b}_{\gamma_0}^{(i)}(\sigma^2 \mathbf{x}))$ for $\mathbf{x} \in [1, L]$, $L = [L/\sigma^2]$.

5.1.3. Propagator, reflection, and transmission. We denote the solution of (5.11) with the initial condition $\mathbf{a}_{\gamma_0}^{(1)}(x=0) = 1, \mathbf{b}_{\gamma_0}^{(1)}(x=0) = 0$ by $(\mathbf{a}_{\gamma_0}^{(1)}(x), \mathbf{b}_{\gamma_0}^{(1)}(x))$. Also, we denote the solution of (5.11) with the initial condition $\mathbf{a}_{\gamma_0}^{(2)}(x=0) = 0, \mathbf{b}_{\gamma_0}^{(2)}(x=0) = 1$ by $(\mathbf{a}_{\gamma_0}^{(2)}(x), \mathbf{b}_{\gamma_0}^{(2)}(x))$.

By linearity of the system (5.7)–(5.8), if $L = [L/\sigma^2]$ and $\sigma^2 \rightarrow 0$, then the mode amplitudes $(a_{\gamma_0}([x/\sigma^2]), b_{\gamma_0}([x/\sigma^2]))_{x \in [0, L]}$ (with (a_γ, b_γ) solution of (5.7)–(5.8) with the boundary conditions (5.9)) converge to $(\mathbf{a}_{\gamma_0}(x), \mathbf{b}_{\gamma_0}(x))_{x \in [0, L]}$, which satisfies

$$(5.16) \quad \begin{pmatrix} \mathbf{a}_{\gamma_0}(x=L) = T \\ \mathbf{b}_{\gamma_0}(x=L) = 0 \end{pmatrix} = \begin{pmatrix} \mathbf{a}_{\gamma_0}^{(1)}(x=L) & \mathbf{a}_{\gamma_0}^{(2)}(x=L) \\ \mathbf{b}_{\gamma_0}^{(1)}(x=L) & \mathbf{b}_{\gamma_0}^{(2)}(x=L) \end{pmatrix} \begin{pmatrix} \mathbf{a}_{\gamma_0}(x=0) = 1 \\ \mathbf{b}_{\gamma_0}(x=0) = R \end{pmatrix},$$

where T and R are the limits of the transmission and reflection coefficients of the surface mode for the randomly perturbed region corresponding to a unit-amplitude right-going surface wave coming from $-\infty$ (i.e., boundary conditions (5.9)).

We can also define the transmission and reflection coefficients corresponding to a unit-amplitude left-going surface wave coming from $+\infty$ (i.e., boundary conditions $b_\gamma(L+1) = \mathbf{1}_{\gamma_0}(\gamma), a_\gamma(0) = 0$):

$$(5.17) \quad \begin{pmatrix} \mathbf{a}_{\gamma_0}(x=L) = \tilde{R} \\ \mathbf{b}_{\gamma_0}(x=L) = 1 \end{pmatrix} = \begin{pmatrix} \mathbf{a}_{\gamma_0}^{(1)}(x=L) & \mathbf{a}_{\gamma_0}^{(2)}(x=L) \\ \mathbf{b}_{\gamma_0}^{(1)}(x=L) & \mathbf{b}_{\gamma_0}^{(2)}(x=L) \end{pmatrix} \begin{pmatrix} \mathbf{a}_{\gamma_0}(x=0) = 0 \\ \mathbf{b}_{\gamma_0}(x=0) = \tilde{T} \end{pmatrix}.$$

The pairs (R, T) and (\tilde{R}, \tilde{T}) have the same distribution because $(\mu_x)_{x=1}^L$ has the same distribution as $(\mu_{L+1-x})_{x=1}^L$. From (5.17) the reflection and transmission coefficients (\tilde{R}, \tilde{T}) are given in terms of $(\mathbf{a}_{\gamma_0}^{(2)}(x=L), \mathbf{b}_{\gamma_0}^{(2)}(x=L))$ as

$$\tilde{R} = \frac{\mathbf{a}_{\gamma_0}^{(2)}(x=L)}{\mathbf{b}_{\gamma_0}^{(2)}(x=L)}, \quad \tilde{T} = \frac{1}{\mathbf{b}_{\gamma_0}^{(2)}(x=L)}.$$

We then find from (5.11) and Itô's formula that, as a function of L , the pair (\tilde{R}, \tilde{T}) is a diffusion process which is a solution of the stochastic differential equation

$$\begin{aligned} d\tilde{R} &= \frac{1}{\sqrt{L_{\text{loc}}}} \left(2i\tilde{R}dW_0(L) - \frac{1}{\sqrt{2}}(1 - \tilde{R}^2)dW_1(L) - \frac{i}{\sqrt{2}}(1 + \tilde{R}^2)dW_2(L) \right) \\ &\quad - \frac{3}{L_{\text{loc}}}\tilde{R}dL - (\lambda + i\kappa)\tilde{R}dL, \\ d\tilde{T} &= \frac{1}{\sqrt{L_{\text{loc}}}} \left(i\tilde{T}dW_0(L) + \frac{1}{\sqrt{2}}\tilde{R}\tilde{T}dW_1(L) - \frac{i}{\sqrt{2}}\tilde{R}\tilde{T}dW_2(L) \right) \\ &\quad - \frac{1}{L_{\text{loc}}}\tilde{T}dL - \frac{1}{2}(\lambda + i\kappa)\tilde{T}dL, \end{aligned}$$

starting from $\tilde{R}(L=0) = 0$ and $\tilde{T}(L=0) = 1$. The application of Itô's formula then gives that the moments of the reflection coefficient $\tilde{\mathcal{R}}_p = \mathbb{E}[|\tilde{R}|^{2p}]$ satisfy the system

$$(5.18) \quad \partial_L \tilde{\mathcal{R}}_p = \frac{p^2}{L_{\text{loc}}} (\tilde{\mathcal{R}}_{p+1} + \tilde{\mathcal{R}}_{p-1} - 2\tilde{\mathcal{R}}_p) - 2\lambda p \tilde{\mathcal{R}}_p,$$

starting from $\tilde{\mathcal{R}}_p(L=0) = \mathbf{1}_0(p)$. This gives the desired result stated in Proposition 4.1.

6. Conclusion. Surface wave propagation across randomly perturbed surfaces of lattices is analyzed in this article. The perturbed constitution of surface associated with the discrete Gurtin–Murdoch model, in contrast to uniform bulk elasticity, is captured by uniform mass and elastic constant for nearest-neighbor interactions parallel to the surface with a finite patch of point mass inhomogeneities. The exact expression for surface wave reflectance and transmittance is provided for every such finite patch of mass perturbation on the surface. The exact semianalytical expressions, as a result of stochastic, multiscale analysis for an ensemble of random mass perturbations, independent and identically distributed with mean zero, form the main result of this article. In the exposition, the cases of weakly and strongly scattering regimes are included, which permit closed form expression for the moments of the radiative loss \mathcal{D} . It is found that the mean value of \mathcal{D} shows distinct types of dependence of its behavior on the assumed structure parameters. In particular, the mean value of \mathcal{D} in the weakly scattering regime is found to be proportional to an effective parameter that depends on the continuous spectrum of the unperturbed system, while in the strongly scattering regime, it is found to depend on another effective parameter but not on the variance of the mass perturbations. The theoretical predictions are supported by illustrations of their excellent agreement with numerical simulations for several choices of surface structure parameters.

Regarding the potential applications of the mathematical analysis of the assumed prototype model, the considerations of this article also apply to electronic transport via edge states in graphene-like structures [49, 25, 46, 3] (see schematic in Figure 8).

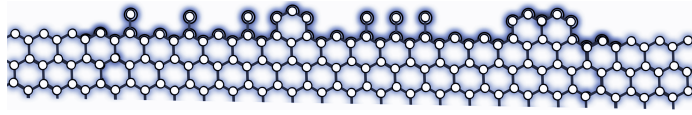


FIG. 8. Schematic of zigzag graphene edge with localized perturbations.

The tight-binding approximation in such a situation, in the presence of surface perturbations, leads to equations similar to the ones analyzed in this article. A detailed and realistic model may not permit an exact theory as developed here, but the qualitative nature of the results is anticipated to be the same; see, for example, [36, 37, 38] for some recent results involving the simplified tight binding models that utilize techniques similar to ones employed in the first part of the article.

Appendix A. Alternative derivation of the normalized eigenbasis. The following is an alternative derivation, using Green's function [43], to obtain the normalized eigenbasis described in section 2.2 for the semi-infinite (reduced) one dimensional lattice model.

Based on (2.8a) and (2.8b), consider

$$(A.1) \quad (\Delta_1 + \omega^2)\psi(\mathbf{y}) = z\psi(\mathbf{y}), \quad \mathbf{y} \in \mathbb{Z}^-,$$

$$(A.2) \quad \psi(\mathbf{y} - 1) - \psi(\mathbf{y}) + m_s\omega^2\psi(\mathbf{y}) = \alpha_s z\psi(\mathbf{y}) - 1, \quad \mathbf{y} = 0.$$

Let

$$(A.3) \quad F_s := (m_s\omega^2 - \alpha_s\gamma - 1).$$

Thus, $\psi(\mathbf{y}) = \psi(0)\ell^{-\mathbf{y}}$, with $(\ell + F_s(z))\psi(0) = -1$, where

$$(A.4) \quad \ell + \ell^{-1} - 2 + \omega^2 = z, \text{ so that } \ell = \frac{1}{2}(z + 2 - \omega^2 \pm \sqrt{(z + 4 - \omega^2)(z - \omega^2)}),$$

and the sign is chosen such that $|\ell| < 1$ when ω is replaced by $\omega + i\varepsilon$ and $\varepsilon > 0$. With the point source at $\mathbf{y} = 0$, in terms of the symbolic use of Green's function, let $\psi(\mathbf{y}) = \mathbf{G}(\mathbf{y}, 0; z)$. Thus,

$$(A.5) \quad \mathbf{G}(\mathbf{y}, 0; z) = \frac{-1}{(\ell + F_s(z))} \ell^{-\mathbf{y}}, \quad \mathbf{y} \leq 0.$$

Also, in terms of the eigenfunctions of \mathcal{L} [43],

$$(A.6) \quad \mathbf{G}(\mathbf{y}, 0; z) = \rho(\gamma_0) \frac{1}{z - \gamma_0} \psi_{\gamma_0}(\mathbf{y}) \bar{\psi}_{\gamma_0}(0) + \int_{\omega^2 - 4}^{\omega^2} d\gamma \rho(\gamma) \frac{1}{z - \gamma} \psi_{\gamma}(\mathbf{y}) \bar{\psi}_{\gamma}(0),$$

i.e., as $\psi_{\gamma}(0) = 1$,

$$(A.7) \quad \mathbf{G}(\mathbf{y}, 0; z) = \rho(\gamma_0) \frac{1}{z - \gamma_0} \psi_{\gamma_0}(\mathbf{y}) + \int_{\omega^2 - 4}^{\omega^2} d\gamma \rho(\gamma) \frac{1}{z - \gamma} \psi_{\gamma}(\mathbf{y}).$$

At $z = \gamma_0$, i.e., at the discrete eigenvalue, the residue

$$(A.8) \quad \text{Res}_{z=\gamma_0} \mathbf{G}(\mathbf{y}, 0; z) = \frac{-1}{(\ell(z) + F_s(z))'} \ell(z)^{-\mathbf{y}}|_{z=\gamma_0}, \quad \mathbf{y} \leq 0,$$

can be simplified to get

$$(A.9) \quad \rho(\gamma_0) = \frac{1}{\alpha_s + 1/(\ell_0^{-2} - 1)}, \quad \psi_{\gamma_0}(\mathbf{y}) = \ell_0^{-y}.$$

For $\gamma \in (\omega^2 - 4, \omega^2)$, i.e., on the continuous band, $\mathbf{G}(\mathbf{y}, 0; \gamma + i0) - \mathbf{G}(\mathbf{y}, 0; \gamma - i0) = -[\frac{1}{(\ell_+ F_s(z))} \ell^{-y}]|_{\gamma-i0}^{\gamma+i0}$, which can be simplified to get $\frac{i}{2\pi} (\mathbf{G}(\mathbf{y}, 0; \gamma + i0) - \mathbf{G}(\mathbf{y}, 0; \gamma - i0)) = \frac{i}{2\pi} \frac{\ell_+ - \ell_+^{-1}}{|\ell_+ + F_s|^2} \psi_\gamma(\mathbf{y})$, leading to

$$(A.10) \quad \rho(\gamma) = -\frac{i}{2\pi} \frac{\ell_+ - \ell_+^{-1}}{|\ell_+ + F_s|^2}.$$

Appendix B. Kolmogorov equations for jump Markov processes. A jump Markov process $(N_x)_{x \geq 0}$ with state space \mathbb{N} is a stepwise constant Markov process which takes values in \mathbb{N} [14, Chapter 6]. Its distribution is characterized by its generator \mathcal{L} , which is of the form

$$(B.1) \quad \mathcal{L}f(n) = \lambda(n) \sum_{k \in \mathbb{N}} Q(n, k) (f(k) - f(n))$$

for any test function f , where for any integer n $\lambda(n) > 0$ and $k \mapsto Q(n, k)$ is a probability distribution on \mathbb{N} (i.e., $Q(n, k) \geq 0$ and $\sum_{k \in \mathbb{N}} Q(n, k) = 1$).

The generator makes it possible to compute any moment of the jump Markov process. Indeed, if we denote $u(x, n) = \mathbb{E}[f(N_x) | N_0 = n]$, then u satisfies the Kolmogorov equation

$$(B.2) \quad \partial_x u = \mathcal{L}u, \quad x > 0,$$

starting from $u(x = 0, n) = f(n)$.

It is also possible to get a probabilistic representation for the solution of an equation of the form

$$(B.3) \quad \partial_x u = \mathcal{L}u - Vu, \quad x > 0,$$

starting from $u(x = 0, n) = f(n)$, where $V : \mathbb{N} \rightarrow [0, +\infty)$. Using the Feynman–Kac representation formula, we have

$$(B.4) \quad u(x, n) = \mathbb{E} \left[f(N_x) \exp \left(- \int_0^x V(N_y) dy \right) | N_0 = n \right].$$

The random dynamics of the jump Markov process $(N_x)_{x \geq 0}$ starting from $N_0 = n$ is as follows:

- Sample a random variable τ_1 with exponential distribution with parameter $\lambda(n)$, sample a random variable Z_1 with the distribution $Q(n, \cdot)$, and set $T_1 = \tau_1$ and

$$(B.5) \quad N_x = n \text{ for } x \in [0, T_1).$$

- For $k \geq 2$, recursively, sample a random variable τ_k with exponential distribution with parameter $\lambda(Z_{k-1})$, sample a random variable Z_k with the distribution $Q(Z_{k-1}, \cdot)$, and set $T_k = T_{k-1} + \tau_k$ and

$$(B.6) \quad N_x = Z_{k-1} \text{ for } x \in [T_{k-1}, T_k).$$

Acknowledgments. The authors thank the anonymous reviewers for their constructive comments and suggestions that helped to improve the manuscript. This work was started during the stay (in March of 2023) of both authors at the Isaac Newton Institute (INI) for Mathematical Sciences, Cambridge. The authors would like to thank INI for support and hospitality during the program “Mathematical theory and applications of multiple wave scattering (MWS),” where work on this paper was undertaken.

REFERENCES

- [1] P. W. ANDERSON, *Absence of diffusion in certain random lattices*, Phys. Rev., 109 (1958), pp. 1492–1505, <https://doi.org/10.1103/PhysRev.109.1492>.
- [2] C. BAKRE AND C. J. LISSENDEN, *Surface roughness effects on self-interacting and mutually interacting Rayleigh waves*, Sensors, 21 (2021), 5495, <https://doi.org/10.3390/s21165495>.
- [3] J. BALDWIN AND Y. HANCOCK, *Effect of random edge-vacancy disorder in zigzag graphene nanoribbons*, Phys. Rev. B, 94 (2016), 165126, <https://doi.org/10.1103/PhysRevB.94.165126>.
- [4] L. BORCEA AND J. GARNIER, *Paraxial coupling of propagating modes in three-dimensional waveguides with random boundaries*, Multiscale Model. Simul., 12 (2014), pp. 832–878, <https://doi.org/10.1137/12089747X>.
- [5] L. BORCEA AND J. GARNIER, *Pulse reflection in a random waveguide with a turning point*, Multiscale Model. Simul., 15 (2017), pp. 1472–1501, <https://doi.org/10.1137/16M1094154>.
- [6] L. BORCEA, J. GARNIER, AND K. SÖLNA, *Onset of energy equipartition among surface and body waves*, Proc. Roy. Soc. A, 477 (2021), 20200775, <https://doi.org/10.1098/rspa.2020.0775>.
- [7] L. BRILLOUIN, *Wave Propagation in Periodic Structures: Electric Filters and Crystal Lattices*, Dover Publications, New York, 1953.
- [8] A. CHAUDHURI, A. KUNDU, D. ROY, A. DHAR, J. L. LEBOWITZ, AND H. SPOHN, *Heat transport and phonon localization in mass-disordered harmonic crystals*, Phys. Rev. B, 81 (2010), 064301, <https://doi.org/10.1103/PhysRevB.81.064301>.
- [9] D. CHEN, G. LV, S. GUO, R. ZUO, Y. LIU, K. ZHANG, Z. SU, AND W. FENG, *Subsurface defect detection using phase evolution of line laser-generated Rayleigh waves*, Optics Laser Technol., 131 (2020), 106410, <https://doi.org/10.1016/j.optlastec.2020.106410>.
- [10] M. V. DE HOOP, J. GARNIER, AND K. SÖLNA, *System of radiative transfer equations for coupled surface and body waves*, Z. Angew. Math. Phys., 73 (2022), 177, <https://doi.org/10.1007/s00033-022-01813-w>.
- [11] K. DRANSFELD AND E. SALZMANN, *Excitation, detection, and attenuation of high-frequency elastic surface waves*, Phys. Acoustics, 7 (1970), pp. 219–272, <https://doi.org/10.1016/B978-0-12-395667-5.50010-6>.
- [12] R. S. EDWARDS, S. DIXON, AND X. JIAN, *Characterisation of defects in the railhead using ultrasonic surface waves*, NDT & E Int., 39 (2006), pp. 468–475, <https://doi.org/10.1016/j.ndteint.2006.01.005>.
- [13] V. A. EREMEYEV AND B. L. SHARMA, *Anti-plane surface waves in media with surface structure: Discrete vs. continuum model*, Int. J. Eng. Sci., 143 (2019), pp. 33–38, <https://doi.org/10.1016/j.ijengsci.2019.06.007>.
- [14] J.-P. FOUQUE, J. GARNIER, G. PAPANICOLAOU, AND K. SÖLNA, *Wave Propagation and Time Reversal in Randomly Layered Media*, Stoch. Model. Appl. Probab. 56, Springer, New York, 2007.
- [15] J. GARNIER AND G. PAPANICOLAOU, *Pulse propagation and time reversal in random waveguides*, SIAM J. Appl. Math., 67 (2007), pp. 1718–1739, <https://doi.org/10.1137/060659235>.
- [16] J. GARNIER AND B. L. SHARMA, *Effective Dynamics in Lattices with Random Mass Perturbations*, preprint, arXiv:2309.03090, 2023.
- [17] D. GASTEAU, N. CHIGAREV, L. DUCOUSO-GANJEHI, V. GUSEV, F. JENSON, P. CALMON, AND V. TOURNAT, *Single crystal elastic constants evaluated with surface acoustic waves generated and detected by lasers within polycrystalline steel samples*, J. Appl. Phys., 119 (2016), 043103, <https://doi.org/10.1063/1.4940367>.
- [18] M. E. GURTIN AND A. IAN MURDOCH, *A continuum theory of elastic material surfaces*, Arch. Ration. Mech. Anal., 57 (1975), pp. 291–323, <https://doi.org/10.1007/BF00261375>.
- [19] M. E. GURTIN AND A. I. MURDOCH, *Surface stress in solids*, Int. J. Solids Struct., 14 (1978), pp. 431–440, [https://doi.org/10.1016/0020-7683\(78\)90008-2](https://doi.org/10.1016/0020-7683(78)90008-2).

- [20] M. S. LORD, M. FOSS, AND F. BESENBACHER, *Influence of nanoscale surface topography on protein adsorption and cellular response*, Nano Today, 5 (2010), pp. 66–78, <https://doi.org/10.1016/j.nantod.2010.01.001>.
- [21] A. A. MARADUDIN, E. W. MONTROLL, G. H. WEISS, AND I. IPATOVA, *Theory of Lattice Dynamics in the Harmonic Approximation*, Solid State Phys. 3, Academic Press, New York, 1971.
- [22] J. MARTIN, C. AUMANN, D. SAVAGE, M. C. TRINGIDES, M. G. LAGALLY, W. MORITZ, AND F. KRETSCHMAR, *Atomic steps on Si(100) surfaces*, J. Vac. Sci. Technol. A, 5 (1987), pp. 615–618, <https://doi.org/10.1116/1.574685>.
- [23] L. MAURER, S. MEI, AND I. KNEZEVIC, *Rayleigh waves, surface disorder, and phonon localization in nanostructures*, Phys. Rev. B, 94 (2016), 045312, <https://doi.org/10.1103/PhysRevB.94.045312>.
- [24] G. MAURYA AND B. L. SHARMA, *Wave scattering on lattice structures involving an array of cracks*, Proc. Roy. Soc. A, 476 (2020), 20190866, <https://doi.org/10.1098/rspa.2019.0866>.
- [25] P. MERINO, H. SANTOS, A. L. PINARDI, L. CHICO, AND J. A. MARTIN-GAGO, *Atomically-resolved edge states on surface-nanotemplated graphene explored at room temperature*, Nanoscale, 9 (2017), pp. 3905–3911, <https://doi.org/10.1039/C7NR00367F>.
- [26] H. MERLITZ, G.-L. HE, C.-X. WU, AND J.-U. SOMMER, *Nanoscale brushes: How to build a smart surface coating*, Phys. Rev. Lett., 102 (2009), 115702, <https://doi.org/10.1103/PhysRevLett.102.115702>.
- [27] R. NOVIKOV AND B. L. SHARMA, *Inverse source problem for discrete Helmholtz equation*, Inverse Problems, 40 (2024), 105005, <https://doi.org/10.1088/1361-6420/ad7054>.
- [28] C. REETZ, R. FISCHER, G. G. ASSUMPCAO, D. P. McNALLY, P. S. BURNS, J. C. SANKEY, AND C. A. REGAL, *Analysis of membrane phononic crystals with wide band gaps and low-mass defects*, Phys. Rev. Appl., 12 (2019), 044027, <https://doi.org/10.1103/PhysRevApplied.12.044027>.
- [29] T. SAKUMA, *Elastic-surface-wave scattering from point-mass defects in a solid surface*, Phys. Rev. B, 8 (1973), pp. 1433–1440, <https://doi.org/10.1103/PhysRevB.8.1433>.
- [30] H.-E. SCHAEFER, *Nanoscience: The Science of the Small in Physics, Engineering, Chemistry, Biology and Medicine*, Springer Science & Business Media, 2010.
- [31] F. SCHILLER, M. RUIZ-OSÉS, J. CORDÓN, AND J. E. ORTEGA, *Scattering of surface states at step edges in nanostripe arrays*, Phys. Rev. Lett., 95 (2005), 066805, <https://doi.org/10.1103/PhysRevLett.95.066805>.
- [32] W. SHABAN AND B. VAINBERG, *Radiation conditions for the difference Schrödinger operators*, Appl. Anal., 80 (2001), pp. 525–556, <https://doi.org/10.1080/00036810108841007>.
- [33] B. L. SHARMA, *Diffraction of waves on square lattice by semi-infinite crack*, SIAM J. Appl. Math., 75 (2015), pp. 1171–1192, <https://doi.org/10.1137/140985093>.
- [34] B. L. SHARMA, *Diffraction of waves on square lattice by semi-infinite rigid constraint*, Wave Motion, 59 (2015), pp. 52–68, <https://doi.org/10.1016/j.wavemoti.2015.07.008>.
- [35] B. L. SHARMA, *On scattering of waves on square lattice half-plane with mixed boundary condition*, Z. Angew. Math. Phys., 68 (2017), 120, <https://doi.org/10.1007/s00033-017-0854-0>.
- [36] B. L. SHARMA, *Electronic transport across a junction between armchair graphene nanotube and zigzag nanoribbon: Transmission in an armchair nanotube without a zigzag half-line of dimers*, European Phys. J. B, 91 (2018), 84, <https://doi.org/10.1140/epjb/e2018-80647-2>.
- [37] B. L. SHARMA, *On electronic conductance of partially unzipped armchair nanotubes: Further analysis*, European Phys. J. B, 92 (2019), 1, <https://doi.org/10.1140/epjb/e2018-90391-2>.
- [38] B. L. SHARMA, *Transmission of waves across atomic step discontinuities in discrete nanoribbon structures*, Z. Angew. Math. Phys., 71 (2020), 73, <https://doi.org/10.1007/s00033-020-01294-9>.
- [39] B. L. SHARMA, *Surface wave across crack-tip in a lattice model*, Philos. Trans. Roy. Soc. A, 380 (2022), 20210396, <https://doi.org/10.1098/rsta.2021.0396>.
- [40] B. L. SHARMA, *Scattering of surface waves by inhomogeneities in crystalline structures*, Proc. Roy. Soc. A, 480 (2024), 20230683, <https://doi.org/10.1098/rspa.2023.0683>.
- [41] B. L. SHARMA AND V. A. EREMEYEV, *Wave transmission across surface interfaces in lattice structures*, Int. J. Eng. Sci., 145 (2019), 103173, <https://doi.org/10.1016/j.ijengsci.2019.103173>.
- [42] I. I. SMOLYANINOV, D. L. MAZZONI, AND C. C. DAVIS, *Imaging of surface plasmon scattering by lithographically created individual surface defects*, Phys. Rev. Lett., 77 (1996), pp. 3877–3880, <https://doi.org/10.1103/PhysRevLett.77.3877>.
- [43] I. STAKGOLD AND M. J. HOLST, *Green's Functions and Boundary Value Problems*, John Wiley & Sons, Hoboken, NJ, 2011.

- [44] R. STEG AND P. KLEMENS, *Scattering of Rayleigh waves by surface defects*, J. Appl. Phys., 45 (1974), pp. 23–29, <https://doi.org/10.1063/1.1662964>.
- [45] F. VARIOLA, J. B. BRUNSKI, G. ORSINI, P. T. DE OLIVEIRA, R. WAZEN, AND A. NANJI, *Nanoscale surface modifications of medically relevant metals: State-of-the art and perspectives*, Nanoscale, 3 (2011), pp. 335–353, <https://doi.org/10.1039/C0NR00485E>.
- [46] K. WAKABAYASHI, S. OKADA, R. TOMITA, S. FUJIMOTO, AND Y. NATSUME, *Edge states and flat bands of graphene nanoribbons with edge modification*, J. Phys. Soc. Jpn., 79 (2010), 034706, <https://doi.org/10.1143/JPSJ.79.034706>.
- [47] R. WALLIS, D. MILLS, AND A. MARADUDIN, *Attenuation of Rayleigh waves by point defects*, Phys. Rev. B, 19 (1979), pp. 3981–3995, <https://doi.org/10.1103/PhysRevB.19.3981>.
- [48] R. F. WALLIS, *Theory of surface modes of vibration in two-and three-dimensional crystal lattices*, Phys. Rev., 116 (1959), pp. 302–308, <https://doi.org/10.1103/PhysRev.116.302>.
- [49] S. WANG, L. TALIRZ, C. A. PIGNEDOLI, X. FENG, K. MÜLLEN, R. FASEL, AND P. RUFFIEUX, *Giant edge state splitting at atomically precise graphene zigzag edges*, Nat. Commun., 7 (2016), 11507, <https://doi.org/10.1038/ncomms11507>.
- [50] Y. WANG, B. RAMIREZ, K. CARPENTER, C. NAIFY, D. C. HOFMANN, AND C. DARAIO, *Architected lattices with adaptive energy absorption*, Extreme Mechanics Lett., 33 (2019), 100557, <https://doi.org/10.1016/j.eml.2019.100557>.